Copy 5

RM A51J19a

NACA

RESEARCH MEMORANDUM

THE EFFECT OF ENTRANCE MACH NUMBER AND LIP SHAPE ON THE SUBSONIC CHARACTERISTICS OF A SCOOP-TYPE-AIR-INDUCTION SYSTEM FOR A SUPERSONIC AIRPLANE

By Curt A. Holzhauser

Ames Aeronautical Laboratory,
Moffett Field, Calif.

NATIONAL ADVISORY COMMITTEE
FOR AERONAUTICS

WASHINGTON
January 9, 1952

NATIONAL ADVISORY COMMITTEE FOR AERONAUTICS

RESEARCH MEMORANDUM

THE EFFECT OF ENTRANCE MACH NUMBER AND LIP SHAPE ON THE SUBSONIC CHARACTERISTICS OF A SCOOP-TYPE AIR-INDUCTION SYSTEM FOR A SUPERSONIC AIRPLANE

By Curt A. Holzhauser

SUMMARY

An experimental investigation was conducted at subsonic speeds to ascertain the effects of lip shape and entrance Mach number on the characteristics of a scoop-type air-induction system designed for an airplane which would fly at supersonic speeds.

The effects of lip shape and entrance Mach number on the ram-recovery ratio at the simulated compressor inlet and on the static pressures on the duct surfaces were investigated for entrance Mach numbers from 0 to choking for free-stream Mach numbers from 0.08 to 0.33 with the model at 0° angle of attack. Measurements of ram-recovery ratio at the simulated compressor inlet were made for the intake with a sharp lip and for the intake with a rounded lip for an angle-of-attack range of -15° to 15° for several mass-flow ratios and several free-stream Mach numbers. The drag of the forward portion of the fuselage with the intakes having sharp lips was compared with that of the same portion of the fuselage with the intakes having rounded lips. This comparison was made for a mass-flow-ratio range of 0 to 2.2 for a free-stream Mach number of 0.24.

At the higher mass-flow ratios the ram-recovery ratio of the intake with the rounded lip was greater than that of the intake with the sharp lip. At a constant mass-flow ratio when the air flow was separated from the duct, the ram-recovery ratio decreased with increasing entrance Mach number, and the internal flow choked at a lower entrance Mach number than was predicted from one-dimensional isentropic-flow relationships. The variation of ram-recovery ratio with angle of attack was less for the intake with the rounded lip than for the intake with the sharp lip.

For a mass-flow ratio of 0.8 and above, the drag coefficients of the forward portion of the fuselage with the intakes having either the rounded lips or the sharp lips were less than the drag coefficient of the forward portion of the faired fuselage.

INTRODUCTION

A twin-scoop air-induction system which was moderately satisfactory at supersonic speeds was developed in the Ames 8- by 8-inch supersonic wind tunnel. The intakes of this installation had sharp leading edges, and they were downstream from the apex of the ogival nose a distance of five forebody diameters. The tests at supersonic speeds (reference 1) indicated minimum total-pressure losses that were approximately equal to those through a normal shock wave at the test Mach numbers of 1.36 to 2.01. An investigation of a similar installation at low subsonic speeds (reference 2) showed that the ram-recovery ratio, measured at the minimum-area station, was above 0.95 for mass-flow ratios below 1.2. However, above a mass-flow ratio of 1.2, the ram-recovery ratio decreased rapidly. Since an airplane utilizing the air-induction system under consideration would be operating at a mass-flow ratio above 2.0 during take-off and climb, this installation would probably be unsatisfactory because of the low ram-recovery ratios at these high mass-flow ratios.

The present investigation was therefore undertaken to compare the ram-recovery ratio and the drag of a supersonic-type intake (sharp lip) with that of a subsonic-type intake (rounded lip) at low subsonic speeds. The effect of entrance Mach number on the ram-recovery ratio of the installation with sharp lips and with rounded lips was studied for subsonic entrance Mach numbers with the model at several angles of attack.

NOTATION

a	speed of sound, feet per second
A	cross-sectional area of duct, square feet
$c_{d'}$	point wake drag coefficient
c_d	section wake drag coefficient
C_D	wake drag coefficient based on frontal area of fuselage at duct station 1

d	duct depth, feet
F	frontal area of fuselage with intakes having sharp lips, measured at duct station 1
g	gravitational constant, 32.2 feet per second per second
H	total pressure, pounds per square foot
$\frac{m_1}{m_o}$	mass-flow ratio $\left(\frac{\rho_1 A_1 V_1}{\rho_o A_1 V_o}\right)$
M_o	free-stream Mach number $\left(\frac{V_o}{a_o}\right)$
M_1	entrance Mach number, based on the duct area 1 inch behind the leading edge of the lip $\left(\frac{W}{a_1 \rho_1 A_1 g}\right)$
p	static pressure, pounds per square foot
P	static-pressure coefficient $\left(\frac{p-p_o}{q_o}\right)$
q	dynamic pressure $\left(\frac{1}{2}\rho V^2\right)$, pounds per square foot
V	velocity of the air stream, feet per second
W	weight rate of air flow (ρAVg), pounds per second
y	perpendicular distance from surface, feet
α	angle of attack measured in the vertical plane of symmetry (plane containing center lines of both ducts), degrees
δ	boundary-layer thickness to where the velocity in the boundary layer is 0.99 of the local velocity outside of the boundary layer, feet
η	diffuser efficiency $\left(1 - \frac{H_2 - H_3}{q_2}\right)$
ρ	mass density of the air, slugs per cubic foot

Subscripts

o	free stream
1	1 inch downstream of duct station 1
2	duct station 2 (minimum-area station)
3	duct station 3 (compressor-inlet station)
m	weighted according to mass flow
a	weighted according to area

DESCRIPTION OF MODEL AND APPARATUS

The proportions of the model were selected to represent an airplane designed for a flight Mach number of 1.7 at an altitude of 28,000 feet using two axial-flow turbojet engines each developing 6000 pounds of static thrust at sea level. The design considerations for the fuselage and air-induction system are discussed in reference 2.

Figure 1 is a photograph of the model in one of the Ames 7- by 10-foot wind tunnels. The intakes were on the top and bottom of the model. A schematic drawing showing the general arrangement of the model is given in figure 2. Figure 3 presents the cross-sectional shapes and the duct areas at duct stations 1, 2, and 3 for the upper half of the fuselage with the intake having a sharp lip. The intakes with the rounded lips had the same cross sections at duct stations 2 and 3. However, at duct station 1 the cross sections differed in the lip thicknesses and ramp widths. (See fig. 4.) The minimum cross-sectional area of the duct was at duct station 2; the ratio of the duct area at this station to that at the station 1 inch downstream of duct station 1 was 0.938.

Figure 4 shows the contours and gives the coordinates of the three lip shapes that were tested. The intake with the sharp leading edge had the same coordinates as the intake tested previously (reference 2). However, the lip of the latter intake had a slightly larger leading-edge radius than that of the lip in the present test, and it did not flex as much at the higher mass-flow ratios. The shapes of the thick and the thin rounded lips were based on a profile found to be satisfactory for submerged intake operation in the research reported in reference 3. Figures 5(a) and 5(b) are photographs of one of the intakes with a sharp leading edge and of one of the intakes with a thick, rounded leading edge, respectively.

The model was mounted on an 8-inch-diameter pipe (fig. 1). The air flow through the model was controlled by a variable-speed centrifugal blower. The quantity of air flow was measured by a standard ASME orifice meter.

Measurements of the total pressure and static pressure at the minimum-area station (duct station 2) were made for the intake having a sharp leading edge. These measurements were made with a total-pressure tube and a static-pressure tube, which were moved in the vertical plane of symmetry. Seventy-six total-pressure tubes and eight static-pressure tubes were used to measure the total-pressure losses and the static-pressure distribution at the simulated compressor inlet (duct station 3). The latter array of tubes was attached to the simulated accessory housing of a turbojet engine.

Flush orifices in the duct floor and duct roof of the installations with the sharp lip and the thick, rounded lip were used to indicate the static pressures on the duct surfaces in the vertical plane of symmetry. Static pressures were also measured on the outer surface of the thick, rounded lip in a similar manner. The location of all the flush orifices are listed in table I.

The wake drag coefficient of the forward portion of the faired fuselage (the fuselage with the intakes sealed and faired as shown in fig. 6), the wake drag coefficient of the forward portion of the fuselage with intakes having sharp leading edges, and the wake drag coefficient of the same portion of the fuselage with the intakes having thick, rounded leading edges were computed from pressures measured with an array of rakes projecting from the external surface of the fuselage at fuselage station 82. This array of rakes, which encompassed more than one-fourth of the perimeter of the fuselage, is shown in figure 7(a). This array was comprised of 17 rakes of 10 total-pressure tubes and 8 rakes of 3 static-pressure tubes. Each rake was perpendicular to the fuselage surface, and the rakes were equally spaced along the perimeter of the fuselage. Plates like the one shown in figure 7(b) were installed on both sides of the fuselage to simulate an image plane. This image plane was used to ascertain whether the drag measured by the installation was affected by the change in external air flow resulting from blocking the bottom duct at the compressor station. All the total-pressure tubes, static-pressure tubes, and surface orifices were connected to water-in-glass or mercury-in-glass multiple-tube manometers. The distributions of pressure indicated on these manometers were recorded photographically.

TESTS

It was reported previously (reference 2) that measurements of ram-recovery ratio and surface static pressures of the top intake and duct of the scoop-type air-induction system tested were unaffected by the air-flow changes resulting from the lower duct being blocked at the compressor station. Therefore, all measurements of ram-recovery ratio and surface static pressures were made using the top duct with the bottom duct blocked at the compressor station.

The ram-recovery ratio at the compressor inlet and the distribution of the pressure ratio, p/H_o, with the various intakes were obtained while the internal flow was varied from 0 to choking. The angle of attack was varied from -15° to 15°. The free-stream Mach number ranged from 0.08 to 0.33 which corresponded to Reynolds numbers of 580,000 to 2,230,000 per foot of length. The ram-recovery ratio was also measured at the minimum-area station in the vertical plane of symmetry of the intake with the sharp lip for free-stream Mach numbers of 0.17 and 0.27 for several mass-flow ratios. The tubes used to make these measurements were removed from the duct whenever they were not being used.

External total-pressure and static-pressure measurements were made at fuselage station 82 with the faired fuselage for a free-stream Mach number of 0.24 and an angle of attack of 0°. These measurements also were made for the fuselage with the intakes having sharp lips and for the fuselage with the intakes having thick, rounded lips for mass-flow ratios from 0 to 2.2 with the bottom duct blocked at the compressor inlet and without the splitter plate installed on the fuselage. The data taken with and without the splitter plate shown in figure 7(b) indicated that the pressure measurements on the upper portion of the fuselage were unaffected by the external air-flow changes resulting from the bottom duct being blocked at the compressor station.

RESULTS

Ram-Recovery Ratio

Presented in figure 8 is the variation of ram-recovery ratio, at the compressor inlet, with mass-flow ratio for the intakes with the sharp lip, the thin, rounded lip and the thick, rounded lip of the test reported herein for a free-stream Mach number of 0.17 with the model at 0° angle of attack. The variation of the ram-recovery ratio with mass-flow ratio of the intake with the sharp lip tested in reference 2 is also presented. The dotted curve in this figure represents the ram-recovery ratio computed for the scoops tested with a negligible entrance

loss and a diffuser efficiency of 0.92. The equation for this curve is derived in the appendix. The ram-recovery ratio with the thick, rounded lip was greater than with the thin, rounded lip at the higher mass-flow ratios; therefore, only two lip shapes are compared in the remainder of the section containing results, the sharp lip and the thick, rounded lip. The latter lip will henceforth be referred to as the rounded or subsonic-type lip.

All values of entrance Mach number and mass-flow ratio presented in this report are average values computed from the weight rate of air flow, and based on the area of the duct 1 inch behind the leading edge of the intake.

The effect of entrance Mach number on the ram-recovery ratio of the intake with the sharp lip and the intake with the rounded lip is shown in figure 9. The effect of entrance Mach number on the variation of ram-recovery ratio with angle of attack is shown in figure 10 for the intakes with both lip shapes for several mass-flow ratios.

The ram-recovery ratios plotted in figures 8, 9, and 10 were computed by weighting the total pressure indicated by each tube according to the area apportioned to it. Another method for averaging ram-recovery ratio is to weight the total-pressure reading of each tube according to the mass of air flowing through the area apportioned to that tube (reference 3). The effect of mass-flow ratio on the difference between the ram-recovery ratios computed by these two methods is shown in figure 11(a) for the intake with the sharp leading edge used in the test reported in reference 2. The effect of entrance Mach number on this difference in ram-recovery ratio is shown in figure 11(b) for the sharp lip and the rounded lip of the present investigation at a mass-flow ratio of approximately 1.6.

The distribution of ram-recovery ratio in the plane of symmetry of the minimum-area station for the intake with the sharp lip is given in figure 12 for several mass-flow ratios for free-stream Mach numbers of 0.17 and 0.27. The distribution of ram-recovery ratio at the compressor inlet is shown in figure 13 for the intakes with both lip shapes for a free-stream Mach number of 0.17 and 0.33 and for mass-flow ratios approaching internal choking.

Static-Pressure Distribution

The surfaces along which the static pressures were measured are indicated by heavy lines on cross-sectional diagrams of the model in figures 14 and 15. The distributions of the pressure ratio, p/H_o,

on these surfaces are presented in figures 14 and 15, respectively, for various mass-flow ratios and several free-stream Mach numbers. The distribution of static-pressure coefficient, P, on the outer surface of the rounded lip is shown in figure 16 for several mass-flow ratios and a free-stream Mach number of 0.17.

The computed relation between the static-pressure coefficient, P, and the pressure ratio, p/H_o, is given in figure 17 for several free-stream Mach numbers.

Drag

The wake drag coefficients of the portion of the faired fuselage forward of station 82 and of the same portions of the fuselages with the subsonic- and the supersonic-type intakes are shown in figure 18. A point wake drag coefficient, c_d', was computed by the method discussed in reference 4 from the local momentum defect in the flow at each total-pressure tube at station 82. This point-drag coefficient was then integrated across the wake for each rake with the resulting value a section wake drag coefficient, $c_d = \frac{1}{x}\int_o^\delta c_d' \, dy$, for each rake. In this equation x is a reference width of 1 foot. An arithmetic summation of the section wake drag coefficients for the entire fuselage at station 82 was made and referenced to the frontal area, F, at duct station 1 of the fuselage with the intakes having sharp lips ($F = 1.05$ sq ft). The resulting value represents the wake drag coefficient for the forward portion of the fuselage. The distributions of section wake drag coefficient are shown in figure 19 for the faired fuselage, for the fuselage with the intakes having sharp lips, and for the fuselage with the intakes having rounded lips. The data are presented for mass-flow ratios of 0.4, 0.6, and 1.0 for a free-stream Mach number of 0.24, with the model at 0° angle of attack.

DISCUSSION

Ram-Recovery Ratio

It is believed that the large differences between the ram-recovery ratio of the intakes with the various lips and that of the theoretical curve shown in figure 8 are the result of separation of the air flow from the inner surface of the intake. Since the effect of a change in mass-flow ratio on the flow around the lip of an intake is comparable to the effect of a change in angle of attack on the air flow over an

airfoil (see accompanying sketch), it is seen that separation of the air flow can occur from the inner surfaces of the intakes tested as the mass-flow ratio is increased. The difference between the ram-recovery ratios of the intakes with the sharp lips was probably caused by the change in flow resulting from the different leading-edge radii and from the flexure of the sharper lip. The remainder of the discussion will pertain to the intakes with the sharper lip and the thick, rounded lip.

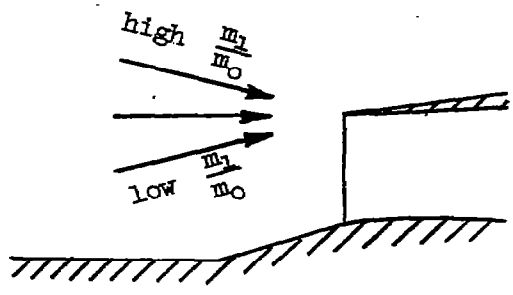

When the entrance Mach number was below 0.5, the total-pressure losses in the vicinity of the duct floor were approximately the same as those in the vicinity of the duct roof at the minimum-area station of the duct with the sharp lip (fig. 12). However, when the entrance Mach number approached the value for choking to occur in the duct, the losses near the duct floor were greater than those near the duct lip. These higher losses in the vicinity of the duct floor apparently did not exist with the intake having a rounded lip since the ram-recovery ratio at the compressor inlet of this intake approximated the ideal ram-recovery ratio shown in figure 8.

Since the ram-recovery ratio of the intake with the sharp leading edge deviated from the ideal values at mass-flow ratios above 1.0 (fig. 8), the air flow probably separated from the surface of the duct. For these mass-flow ratios the ram-recovery ratio decreased with increasing entrance Mach number (fig. 9(a)). For mass-flow ratios below 1.0 the effect of entrance Mach number on the ram-recovery ratio was small. At a mass-flow ratio of 1.6 the internal flow choked at an entrance Mach number of 0.62. As the mass-flow ratio was increased to 2.1 by decreasing the free-stream Mach number, the effective minimum cross-sectional area of the duct was probably further reduced by increased air-flow separation, and the flow choked at an entrance Mach number of 0.58. Since the ram-recovery ratio of the intake with the rounded lip approximated the ideal values, the air flow probably did not separate from this duct; and the effect of entrance Mach number on the ram-recovery ratio was small within the Mach-number range for which the data are presented (fig. 9(b)). The entrance Mach number for choking in this intake was approximately 0.73 for all the mass-flow ratios shown in figure 9(b). For the area ratio of the installation tested, the entrance Mach number for internal choking would be 0.74 if the entering boundary layer were negligible and if the flow were one-dimensional isentropic (reference 5).

The high total-pressure losses at high mass-flow ratios may be avoided by the use of auxiliary air inlets which operate only when large air-flow quantities are required at low forward speeds.

In figure 10, it is seen that the variation of ram-recovery ratio with angle of attack was smaller for the rounded lip than for the sharp lip. In reference 2 it was shown that for the top intake of the scoop-type installation with the sharp lip the variation of ram-recovery ratio with angle of attack was small as compared to the variation of ram-recovery ratio with angle of sideslip. The small variation of ram-recovery ratio with angle of attack was the result of vortices which formed from the forebody and reduced the boundary-layer thickness when the model was at an angle of attack.

Static-Pressure Distribution

It is evident from the static-pressure distribution on the outer surface of the rounded lip (fig. 16) that the effect of a change in mass-flow ratio on the air flow around the lip of an intake is similar to the effect of a change in angle of attack on the air flow over an airfoil. At a mass-flow ratio of 1.6 (where separation did not exist on the outer surface of the lip), the static pressures were constant and approximately equal to the free-stream static pressure. As the mass-flow ratio was decreased to 1.0, a minimum pressure peak developed near the leading edge. With a further decrease in mass-flow ratio to 0.4, separation occurred on the outer surface as was indicated by the increase in the minimum static pressure near the leading edge and a decrease in the pressure coefficient farther downstream. The low static pressures that occurred at a mass-flow ratio of 1.0 could adversely affect the drag of the installation at high subsonic speeds. However, the lip shape can be altered slightly to eliminate these low static pressures near the leading edge and still retain the original pressure-recovery characteristics (reference 6).

At entrance Mach numbers corresponding to choked flow in the duct, a complex supersonic flow existed in the duct between 2 and 8 inches from the leading edge of the intake with the sharp lip (fig. 14). The maximum local Mach number corresponding to the minimum pressure ratio of 0.29 in this region can be computed as 1.4 if the total-pressure losses back to this area are neglected (reference 5). For the intake with the rounded leading edge, existence of supersonic flow in the duct was indicated by pressure ratios less than 0.53 at the high entrance Mach numbers in the vicinity of 8 inches from the leading edge (fig. 15). The maximum local Mach number corresponding to the minimum pressure ratio was 1.2. At equivalent entrance Mach numbers, assuming negligible total-pressure losses, the regions of supersonic flow extended over a

smaller portion of the duct for the intake having a rounded lip than for the intake having a sharp lip.

Drag

The wake drag coefficient of the forward portion of the fuselage with the intakes having sharp leading edges increased rapidly with decreasing mass-flow ratio below a mass-flow ratio of 0.8. Above a mass-flow ratio of 1.0 the wake drag coefficient changed only slightly (fig. 18). Tuft studies indicated that below a mass-flow ratio of 0.8 the air flow separated from the outer surface of the sharp lip at the leading edge. This type of air-flow separation is common with thin airfoils at moderate angles of attack and is accompanied by large increments of drag. Above a mass-flow ratio of about 1.0 the reduction in wake drag coefficient probably was caused by the thinning of the fuselage boundary layer behind the intake as the mass-flow ratio was increased. For a mass-flow ratio of 0.7, the wake drag coefficient of the forward portion of the fuselage with the intakes having sharp leading edges was approximately equal to the wake drag coefficient of the corresponding portion of the faired fuselage.

Tuft studies and an analysis of the pressure distribution on the rounded lip indicated that the air flow separated from the outer surface of the lip for mass-flow ratios below 0.7. At each mass-flow ratio of this test the wake drag coefficient of the forward portion of the fuselage with the intakes having rounded lips was greater than the wake drag coefficient of the forward portion of the fuselage with the intakes having sharp lips. Above a mass-flow ratio of 0.8 the wake drag coefficients of the forward portion of the fuselage with the intakes having either the rounded lips or the sharp lips were less than that of the corresponding portion of the faired fuselage.

CONCLUSIONS

The following conclusions were drawn from the results of the experimental investigation reported herein:

1. For subsonic Mach numbers and high mass-flow ratios, the ram-recovery ratio of the intake with the rounded lip was greater than that of the intake with the sharp lip.

2. When the air flow was not separated from the inner surfaces of the intake near its leading edge, the entrance Mach number for choking in the duct was approximated by one-dimensional isentropic flow relationships. At a constant mass-flow ratio with no air-flow

separation from the inner surface of the intake and up to a choking Mach number, the ram-recovery ratio was changed very little by changes in the subsonic entrance Mach number of this investigation.

3. When the air flow was separated from the inner surface of the intake near its leading edge, the flow choked at a lower entrance Mach number than was predicted from isentropic-flow relationships. At a constant mass-flow ratio for the condition of separated flow, the ram-recovery ratio decreased with increasing entrance Mach number.

4. The variation of ram-recovery ratio with angle of attack was less for the air-induction system with the rounded lip than with the sharp lip.

5. At mass-flow ratios of 0.8 and above, the wake drag coefficients of the forward portion of the fuselage with the intakes having either the rounded lips or the sharp lips were less than that of the corresponding portion of the faired fuselage.

Ames Aeronautical Laboratory,
National Advisory Committee for Aeronautics,
Moffett Field, Calif.

APPENDIX

IDEAL RAM-RECOVERY RATIO AT THE COMPRESSOR INLET OF THE AIR-INDUCTION SYSTEM TESTED

The ram-recovery ratio at the compressor inlet of an air-induction system is equal to the ram-recovery ratio at the minimum-area station minus the losses in the diffuser, thus,

$$\frac{H_3-p_o}{H_o-p_o} = \frac{H_2-p_o}{H_o-p_o} - \frac{H_2-H_3}{H_o-p_o} \tag{1}$$

For incompressible flow $q_o = H_o - p_o$, then,

$$\frac{H_3-p_o}{H_o-p_o} = \frac{H_2-p_o}{H_o-p_o} - \left(\frac{H_2-H_3}{q_2}\right)\left(\frac{q_2}{q_o}\right) \tag{2}$$

If the losses at the entrance of the duct and the losses between duct stations 1 and 2 are negligible, as was noted for mass-flow ratios between 0.2 and 1.2 for the sharp lip of reference 2, equation (2) becomes

$$\frac{H_3-p_o}{H_o-p_o} = 1 - (1-\eta)\frac{q_2}{q_o} \tag{3}$$

where η is the diffuser efficiency $1 - \frac{H_2-H_3}{q_2}$

For incompressible, adiabatic flow

$$\frac{V_1}{V_o} = \frac{m_1}{m_o}$$

and

$$\frac{V_1}{V_2} = \frac{A_2}{A_1}$$

Consequently, equation (3) becomes

$$\frac{H_3-p_o}{H_o-p_o} = 1 - (1-\eta)\left(\frac{A_1}{A_2}\right)^2\left(\frac{m_1}{m_o}\right)^2 \qquad (4)$$

In reference 2, it was noted that the variation of diffuser efficiency with mass-flow ratio was small, and that the average diffuser efficiency was approximately 0.92. For this diffuser efficiency, for negligible entrance losses, and with no separation in the duct, the variation of ram-recovery ratio with mass-flow ratio for the installation tested would be represented by the following equation:

$$\frac{H_3-p_o}{H_o-p_o} = 1 - 0.091\left(\frac{m_1}{m_o}\right)^2 \qquad (5)$$

The parabolic curve representing this equation is plotted in figure 8 as a dotted line.

REFERENCES

1. Davis, Wallace F., Edwards, Sherman S., and Brajnikoff, George B.: Experimental Investigation at Supersonic Speeds of Twin-Scoop Duct Inlets of Equal Area. IV – Some Effects of Internal Duct Shape Upon an Inlet Enclosing 37.2 Percent of the Forebody Circumference. NACA RM A9A31, 1949.

2. Holzhauser, Curt A.: An Experimental Investigation at Subsonic Speeds of a Scoop-Type Air-Induction System for a Supersonic Airplane. NACA RM A51E24, 1951.

3. Mossman, Emmet A., and Randall, Lauros M.: An Experimental Investigation of the Design Variables for NACA Submerged Duct Entrances. NACA RM A7I30, 1948.

4. Baals, Donald D., and Mourhess, Mary J.: Numerical Evaluation of the Wake-Survey Equations for Subsonic Flow Including the Effect of Energy Addition. NACA ARR L5H27, 1945.

5. Staff of the Ames 1- by 3-foot Supersonic Wind-Tunnel Section: Notes and Tables for Use in the Analysis of Supersonic Flow. NACA TN 1428, 1947.

6. Watson, Earl C.: Some Low-Speed Characteristics of an Air-Induction System Having Scoop-Type Inlets With Provisions for Boundary-Layer Control. NACA RM A51F15, 1951.

TABLE I. – LOCATION OF PRESSURE ORIFICES

[Distance Downstream of Duct Station 1 in inches]

Duct Floor	Duct Roof	Outer Surface of Lip
-4.00	0[a]	0.06[a]
-2.00	.06[a]	.13[a]
0	.13[a]	.25[a]
1.00	.25[a]	.50[a]
2.00	.50[a]	1.00[a]
3.00	1.00[a]	
4.00	2.00[a]	
6.00	3.00	
8.00	4.00	
10.00	6.00	
12.00	8.00	
14.00	10.00	
16.00	12.00	
18.00	14.00	
20.00	16.00	
22.00	18.00	
24.00	20.00	
26.00	22.00	
28.00	24.00	
30.13	26.00	
	28.00	
	30.13	

[a]Orifices only on intake with rounded leading-edge.

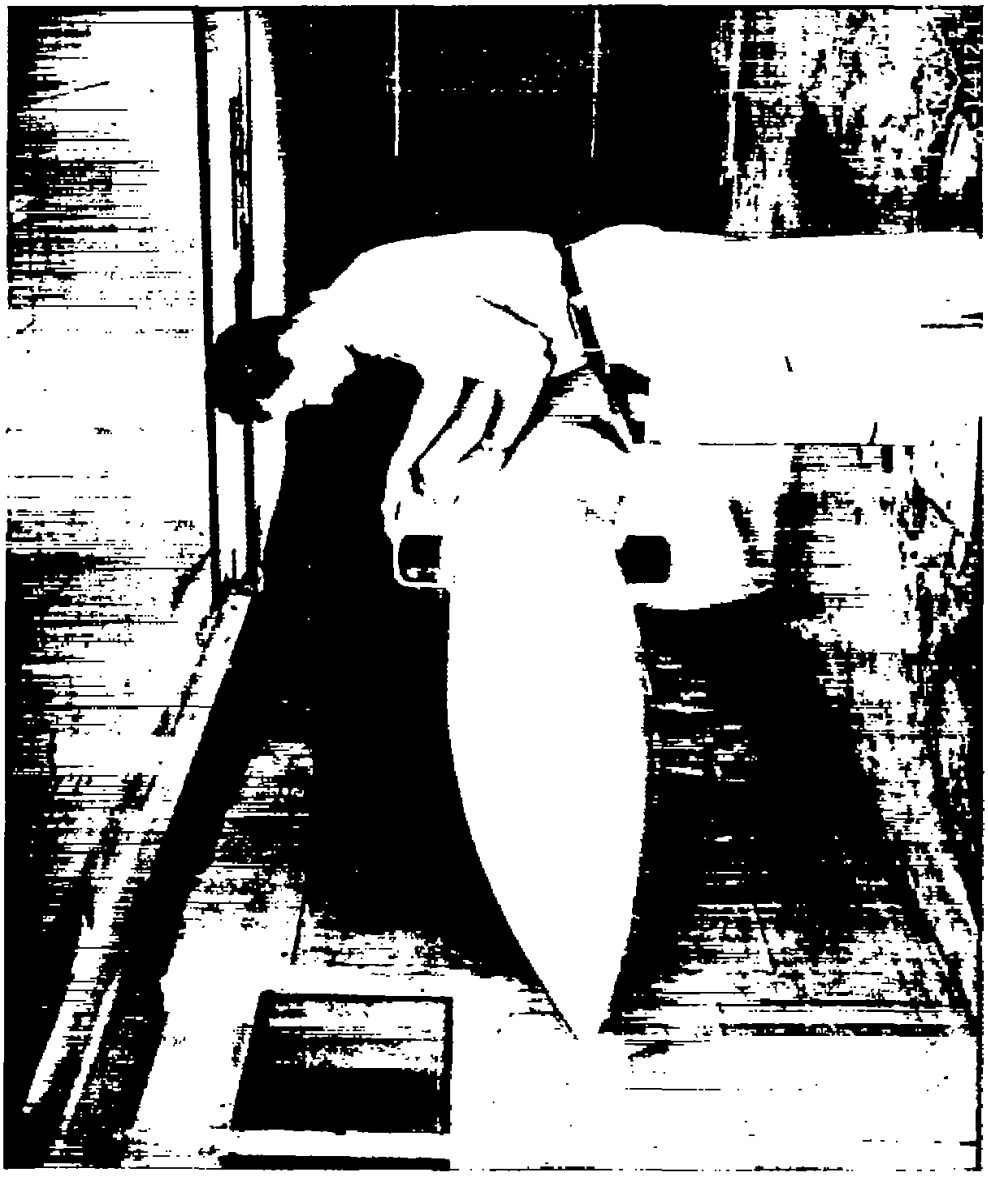

Figure 1.- The model with the intakes.

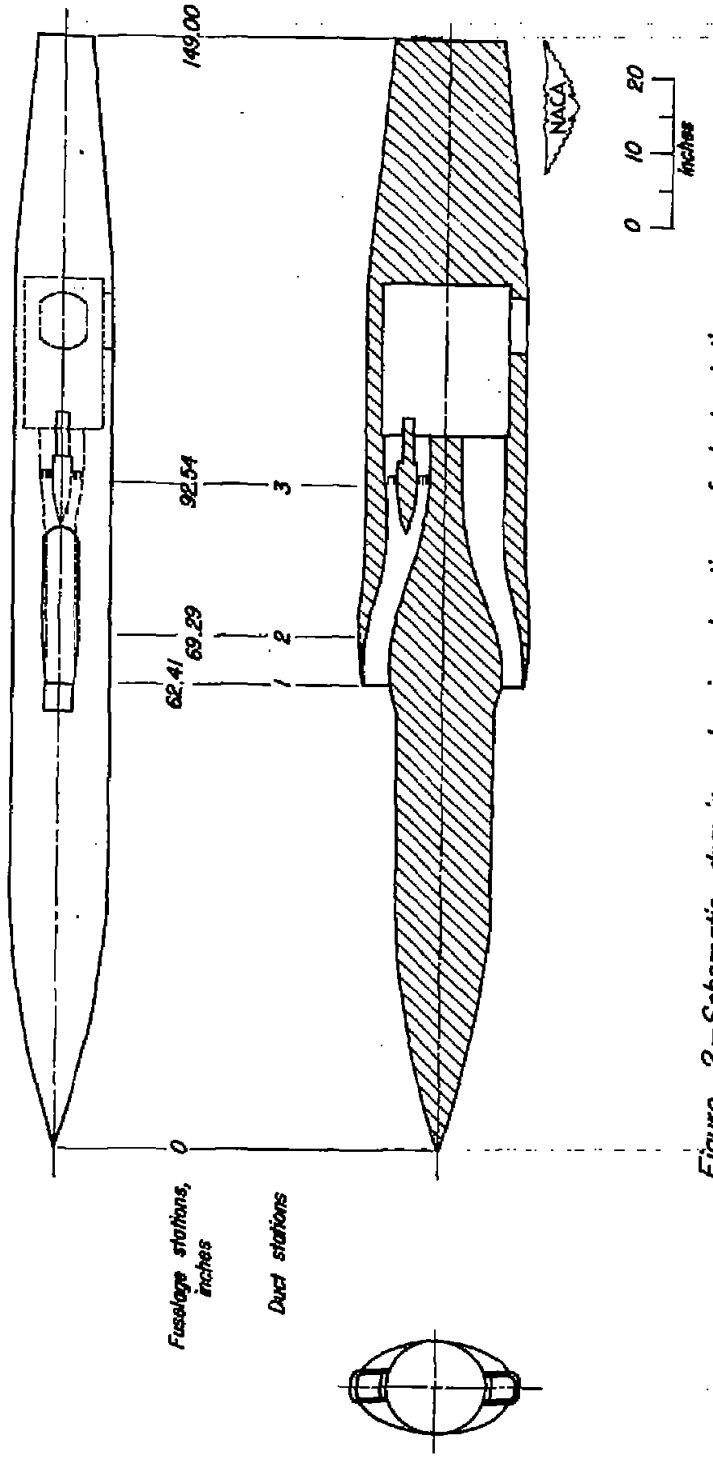

Figure 2.—Schematic drawing showing location of duct stations.

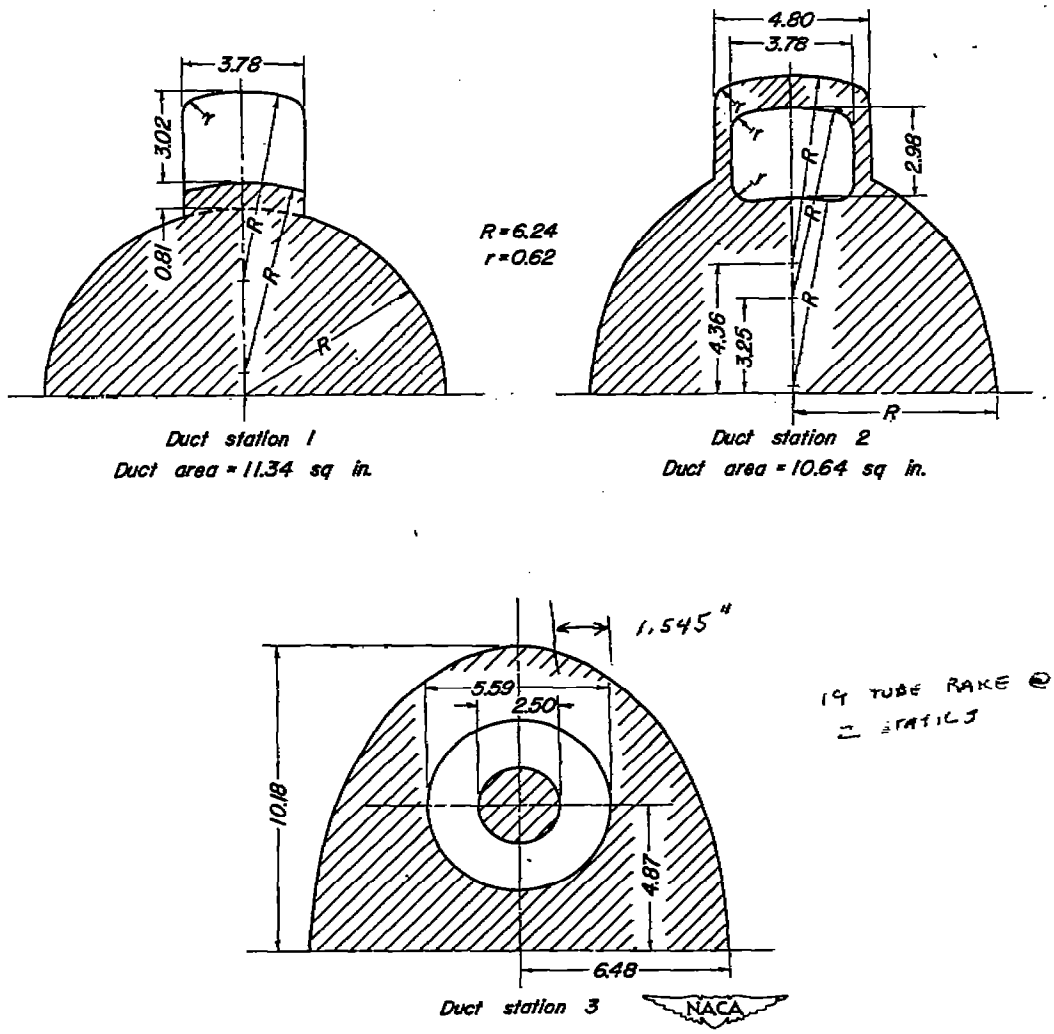

Figure 3.—Cross sections and duct areas at duct stations 1, 2, and 3 for the intake with the sharp lip.

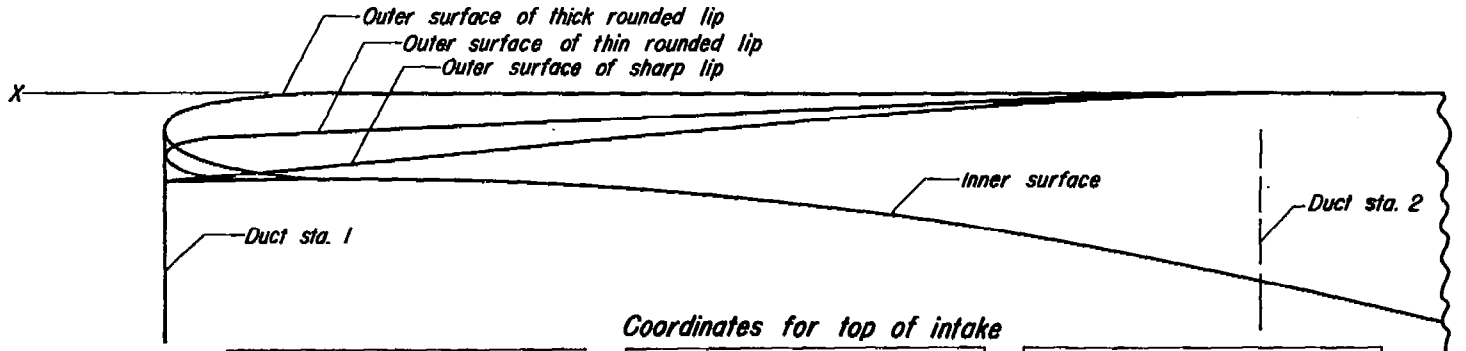

Coordinates for top of intake

Sharp lip		
Distance from duct station 1	From X to inner surface	From X to outer surface
0	0.518	0.518
2.293	.515	.317
4.587	.718	.117
6.880	1.107	0

Width of ramp 3.780 inches

Thin rounded lip		
Distance from duct station 1	From X to inner surface	From X to outer surface
0	0.365	0.365
0.050	.426	.311
.100	.449	.298
.200	.479	.276
.300	.499	.265
.400	.507	.257
.500	.510	.251
2.293	.515	.173
4.587	.713	.073
6.880	1.107	0

Width of ramp 4.072 inches

Thick rounded lip		
Distance from duct station 1	From X to inner surface	From X to outer surface
0	0.209	0.209
0.050	.292	.125
.100	.326	.101
.200	.372	.076
.300	.409	.057
.400	.438	.041
.500	.460	.026
.600	.475	.016
.700	.488	.007
.800	.496	.003
.900	.501	0
1.000	.510	0
2.293	.515	0
4.587	.713	0
6.880	1.107	0

Width of ramp 4.382 inches

Note: All dimensions are in inches.

Coordinates of inner and outer surfaces of the sides of the intake were the same as for the top of the intake except inner surface was parallel to X aft of one inch from duct station 1.

NACA

Figure 4.– Coordinates of the lips.

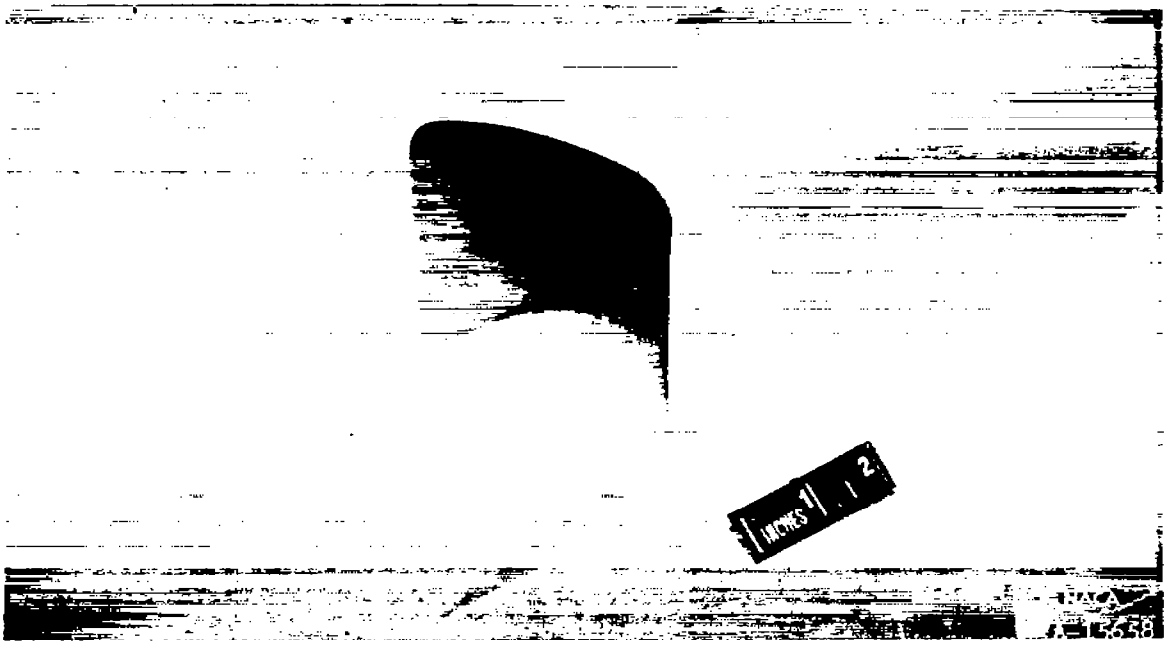

(a) Sharp lip (supersonic type).

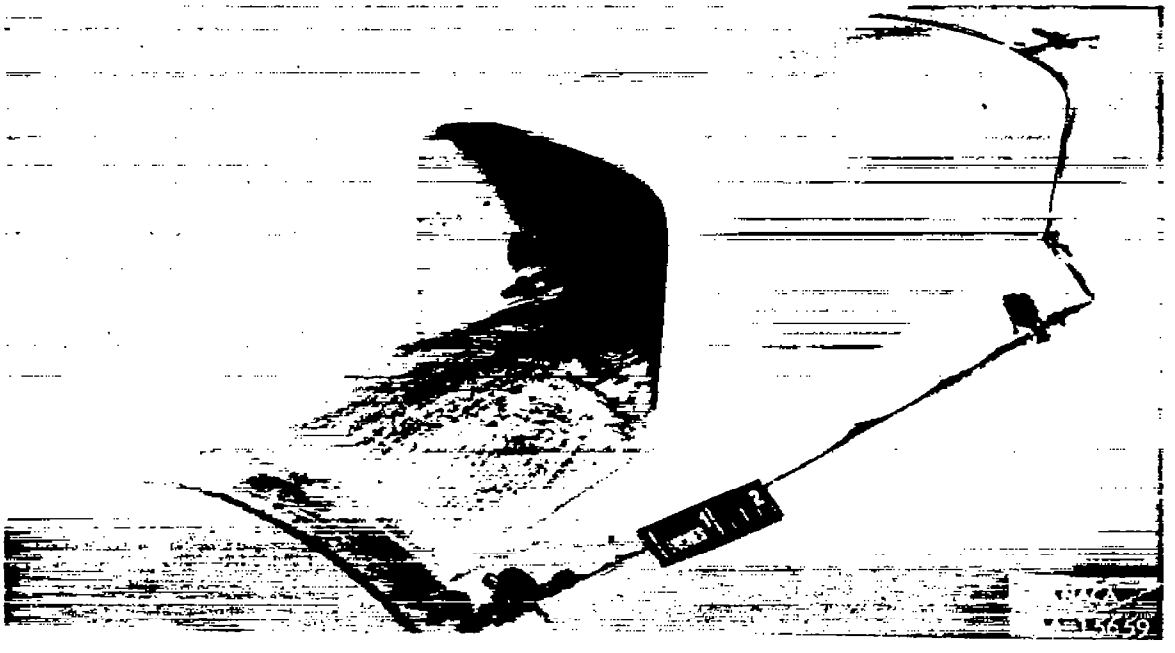

(b) Thick, rounded lip (subsonic type).

Figure 5.- Two of the intakes investigated.

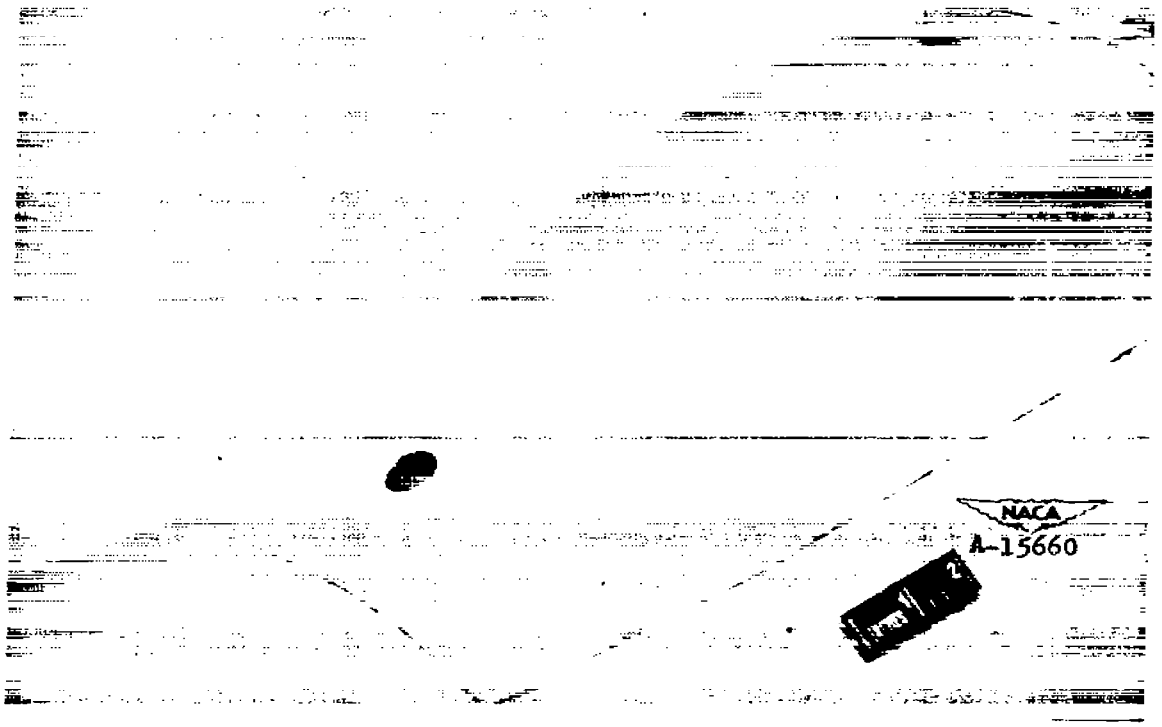

Figure 6.- The intake faired and sealed to form the faired fuselage.

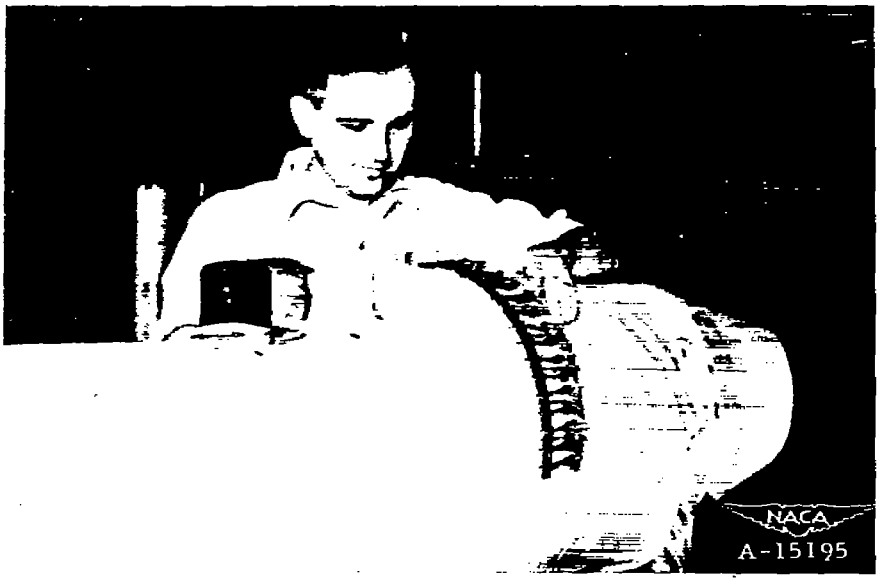

(a) The array of rakes used to measure drag.

(b) Plate dividing upper half of fuselage from lower half.

Figure 7.- Apparatus used to determine wake drag.

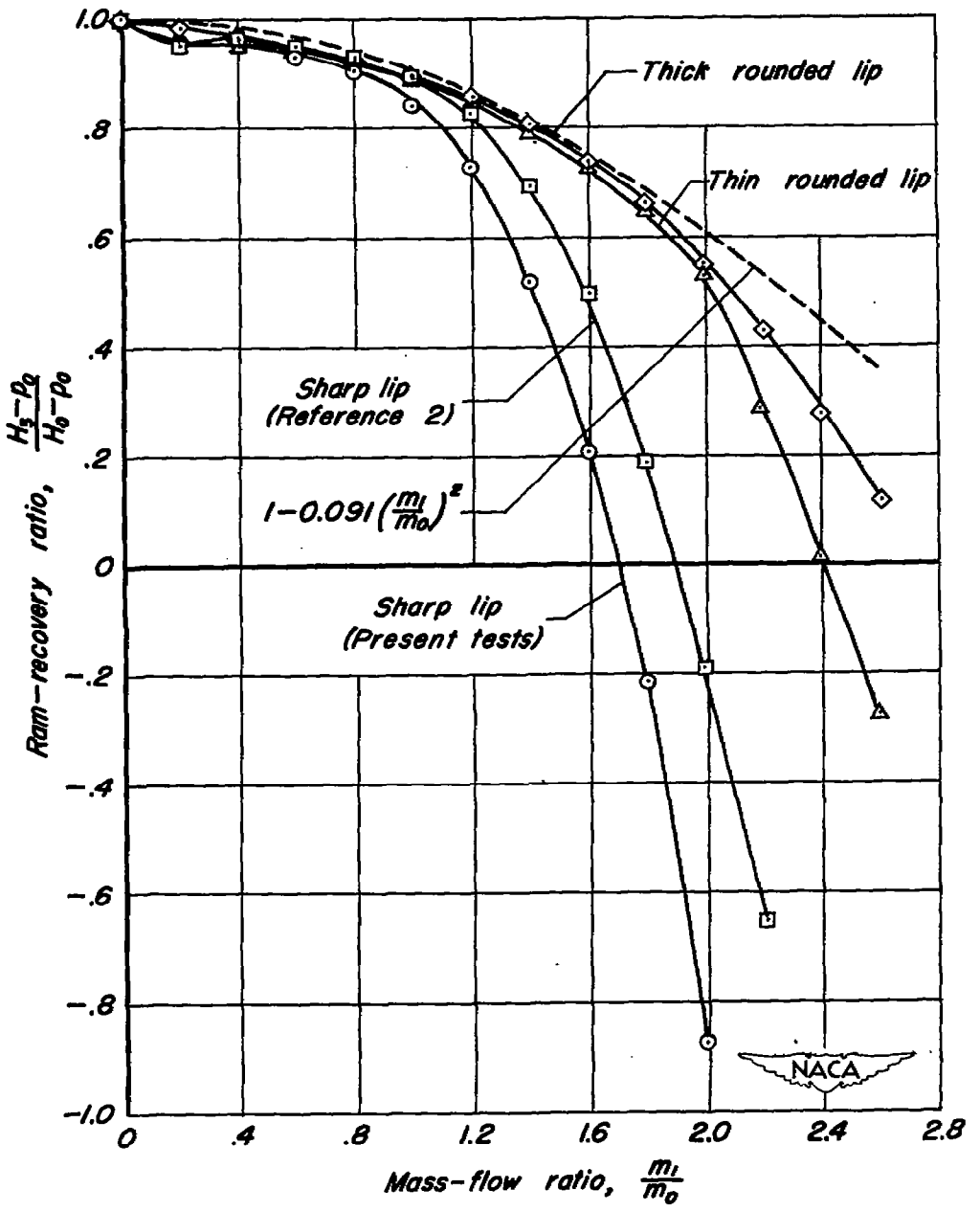

Figure 8.—The variation of ram-recovery ratio with mass-flow ratio. $M_0 = 0.17$, $\alpha = 0°$.

CONFIDENTIAL

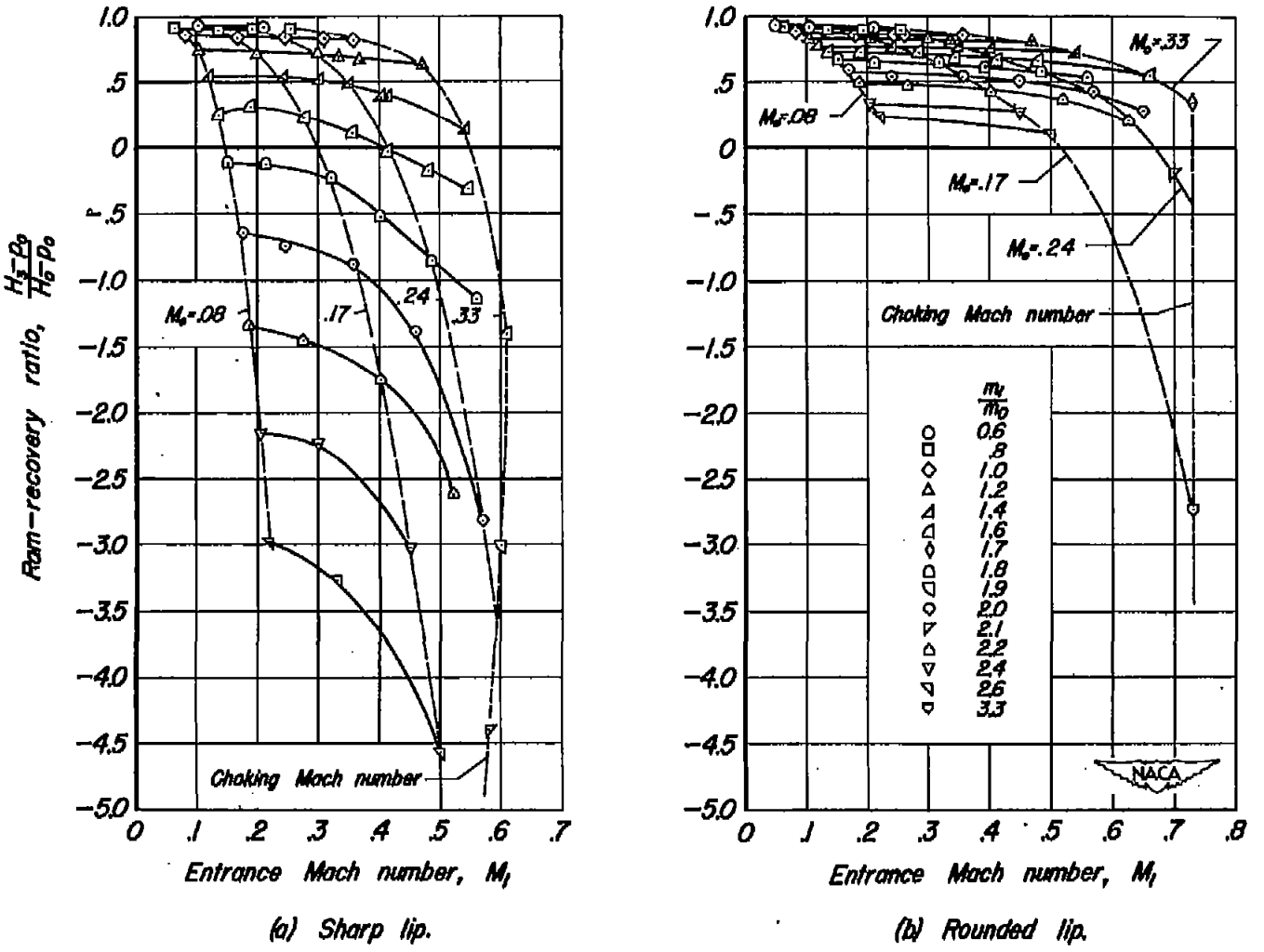

(a) Sharp lip.

(b) Rounded lip.

Figure 9.–The variation of ram-recovery ratio with entrance Mach number for $\alpha = 0°$.

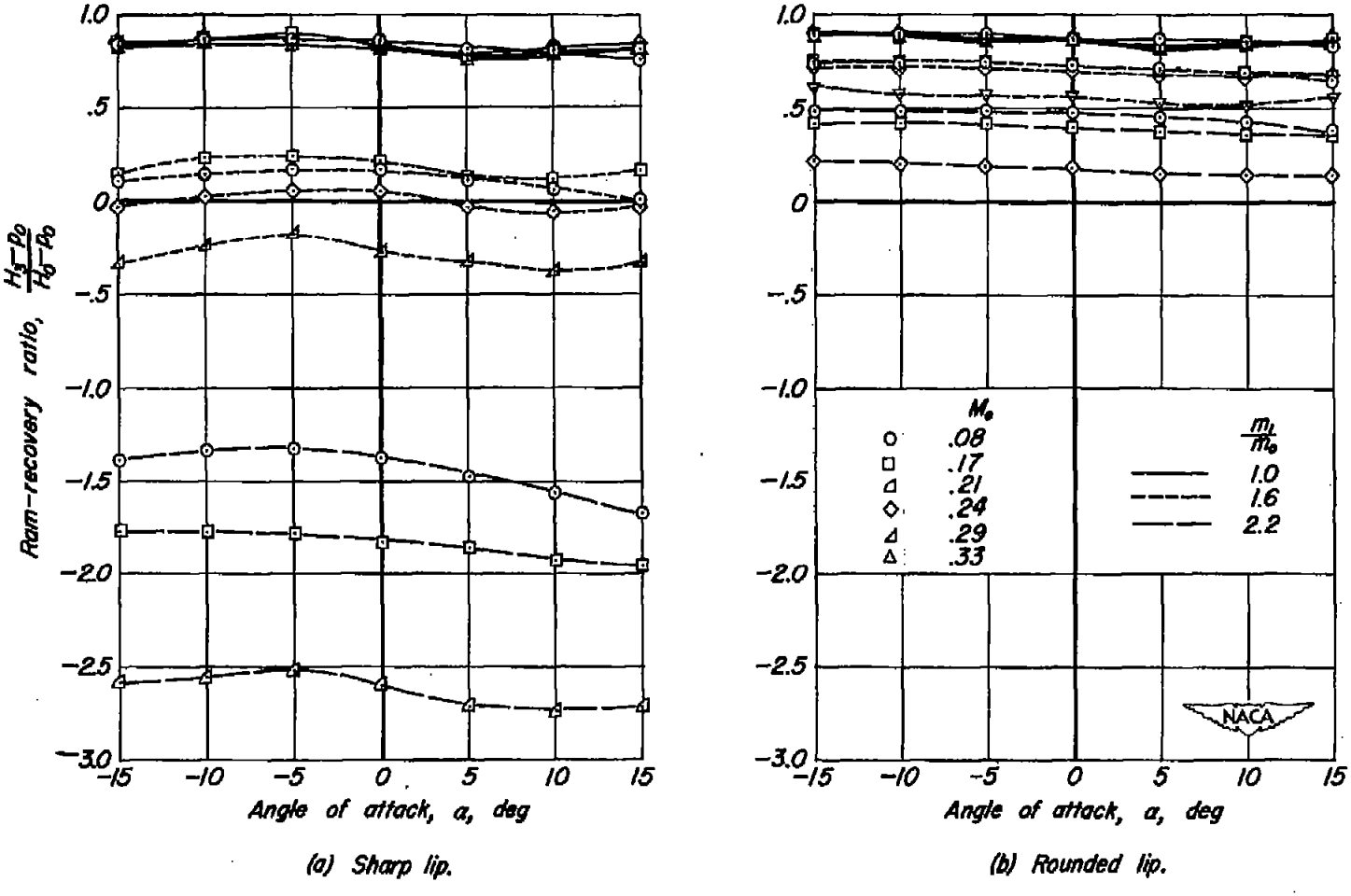

Figure 10.--The variation of ram-recovery ratio with angle of attack.

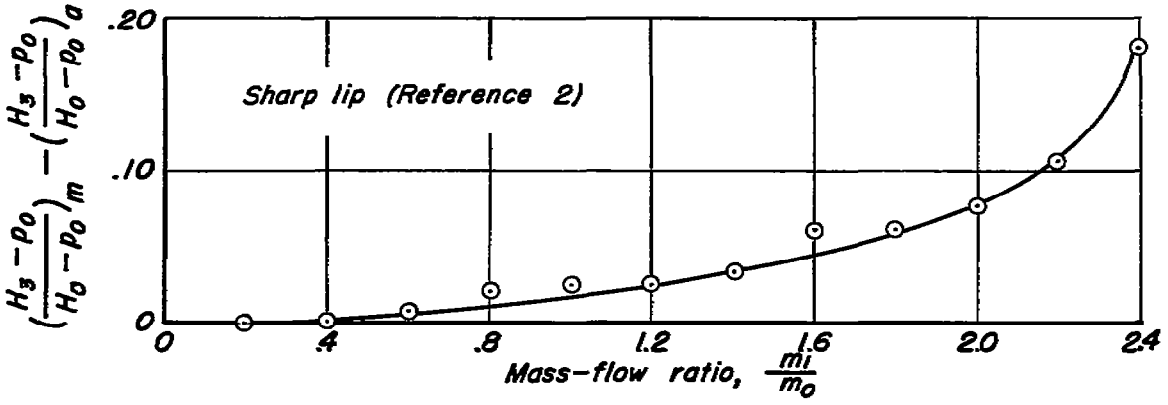

(a) Effect of mass-flow ratio. $M_0 = 0.17$.

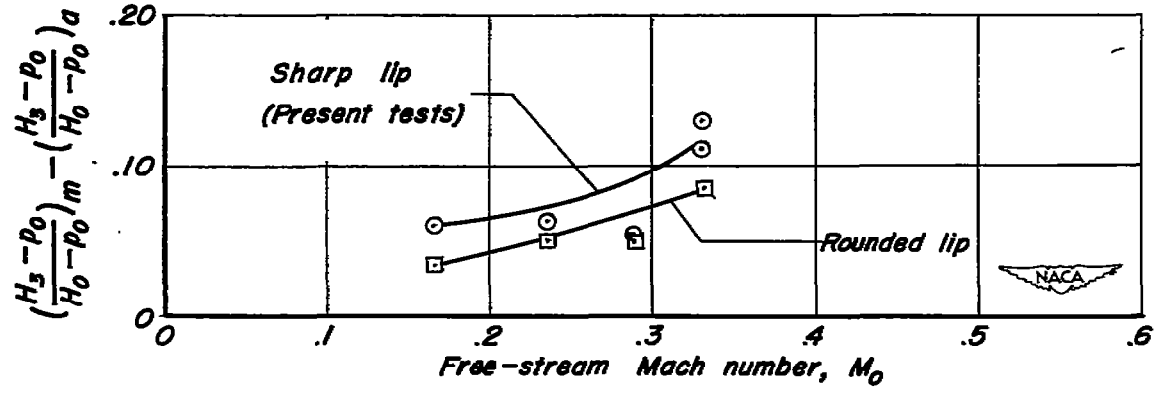

(b) Effect of Mach number. $\frac{m_i}{m_0} = 1.6$.

Figure 11.—The effect of mass-flow ratio, Mach number, and lip shape on the difference between the ram-recovery ratio weighted according to mass-flow and according to area. $\alpha = 0°$.

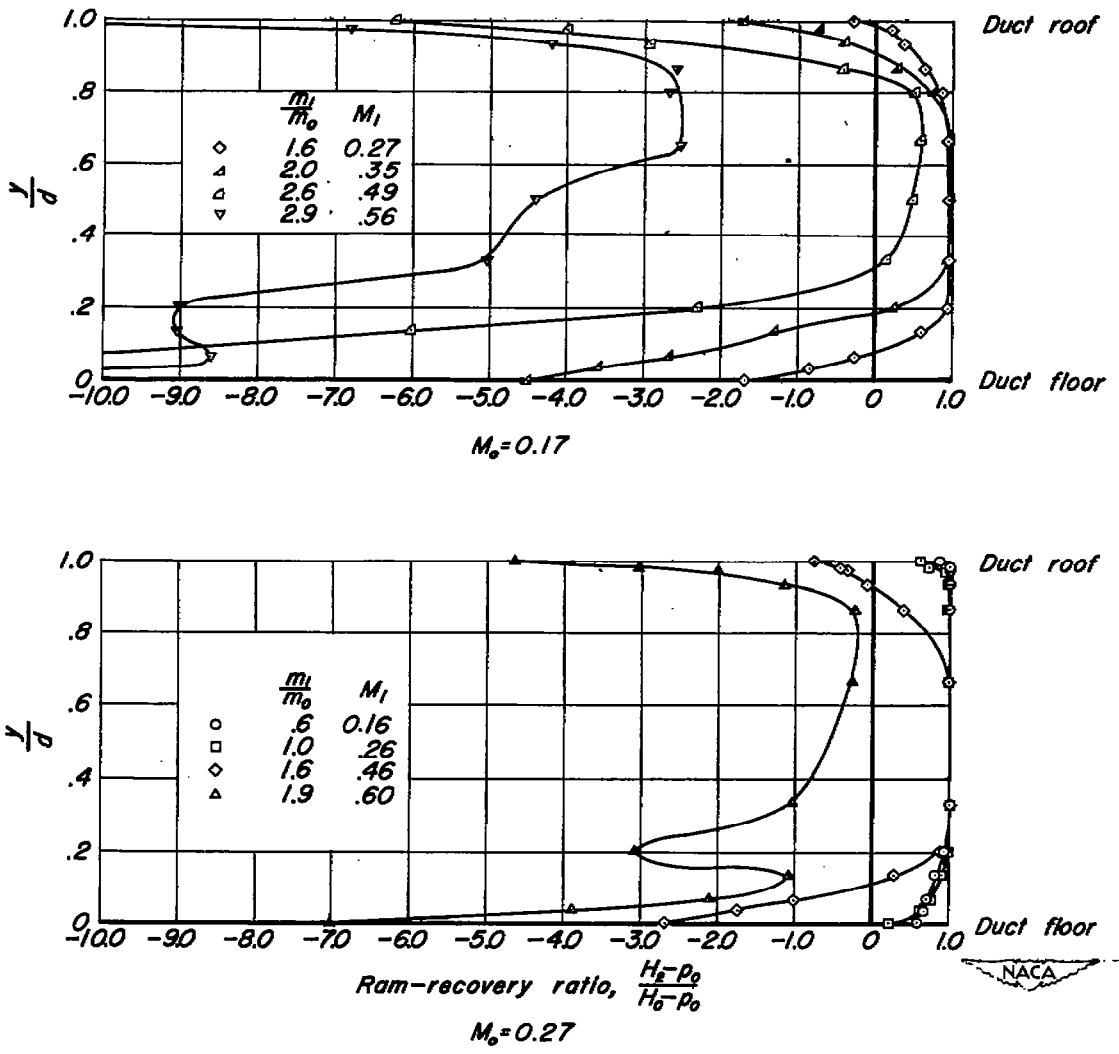

Figure 12.— Distribution of the ram-recovery ratio in the plane of symmetry of the minimum-area station for the intake with the sharp lip. $\alpha = 0°$

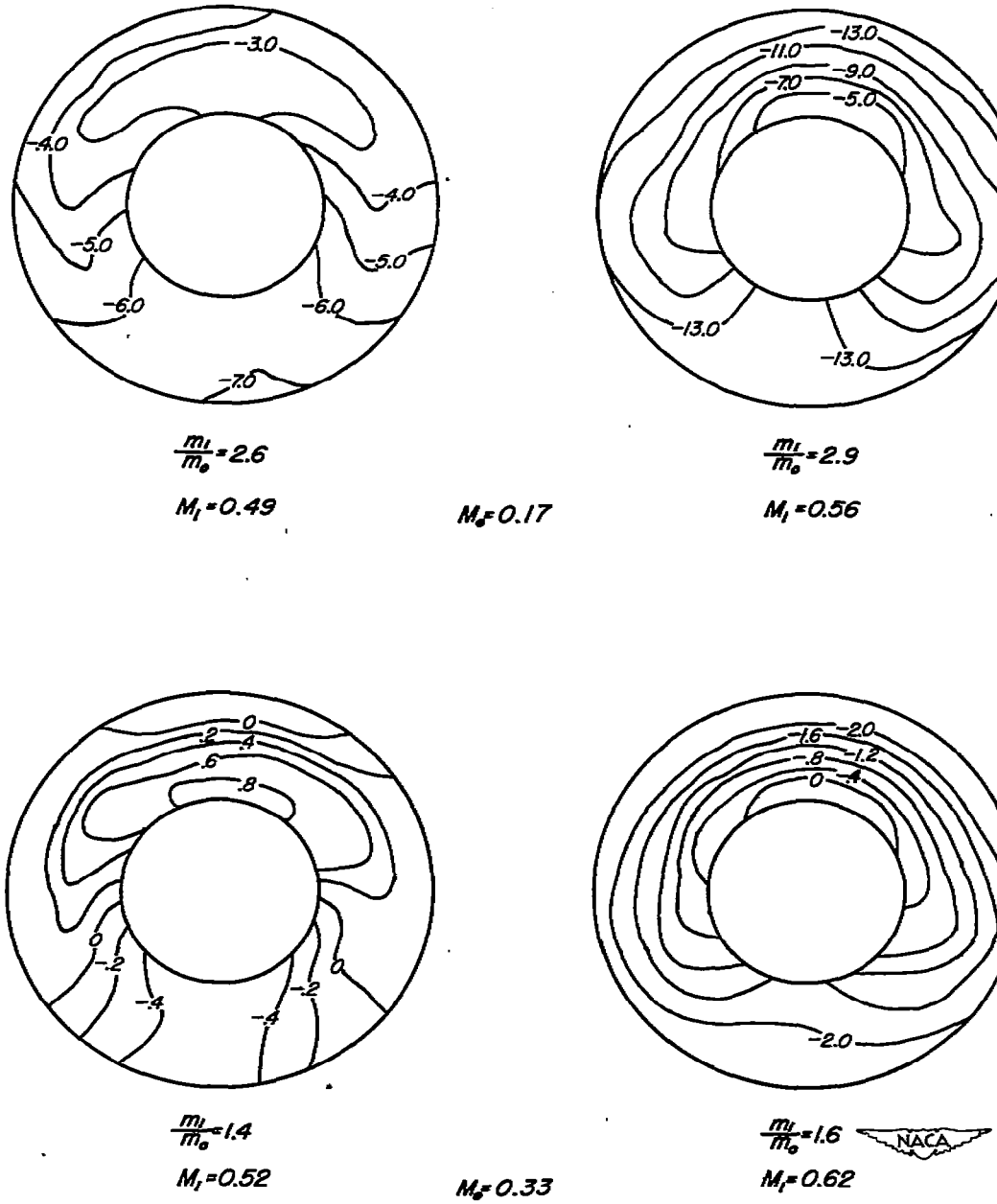

$\frac{m_1}{m_0}$=2.6 M_1=0.49 M_0=0.17 $\frac{m_1}{m_0}$=2.9 M_1=0.56

$\frac{m_1}{m_0}$=1.4 M_1=0.52 M_0=0.33 $\frac{m_1}{m_0}$=1.6 M_1=0.62

(a) Sharp lip.

Figure 13.—Distribution of ram-recovery ratio at the compressor inlet, as viewed looking upstream. $\alpha=0°$.

[redacted]

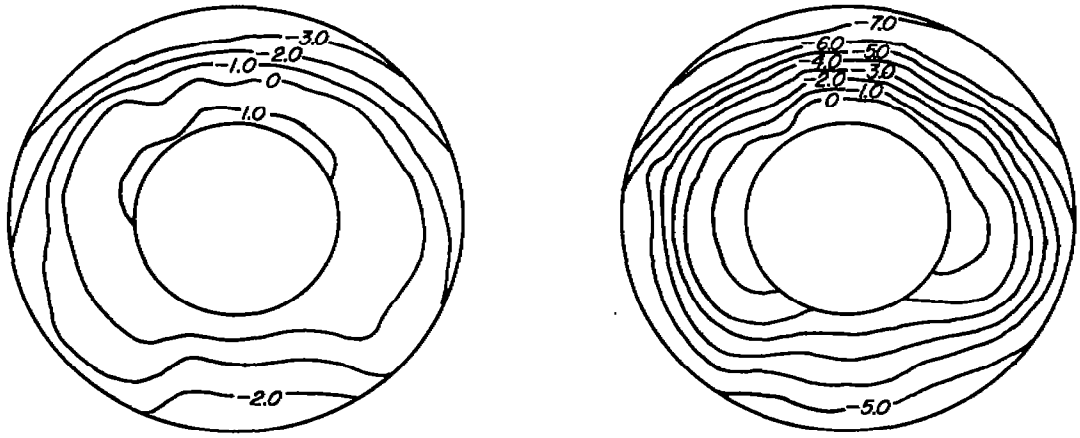

$\frac{m_1}{m_o} = 3.0$
$M_1 = 0.60$

$\frac{m_1}{m_o} = 3.3$
$M_1 = 0.73$

$M_o = 0.17$

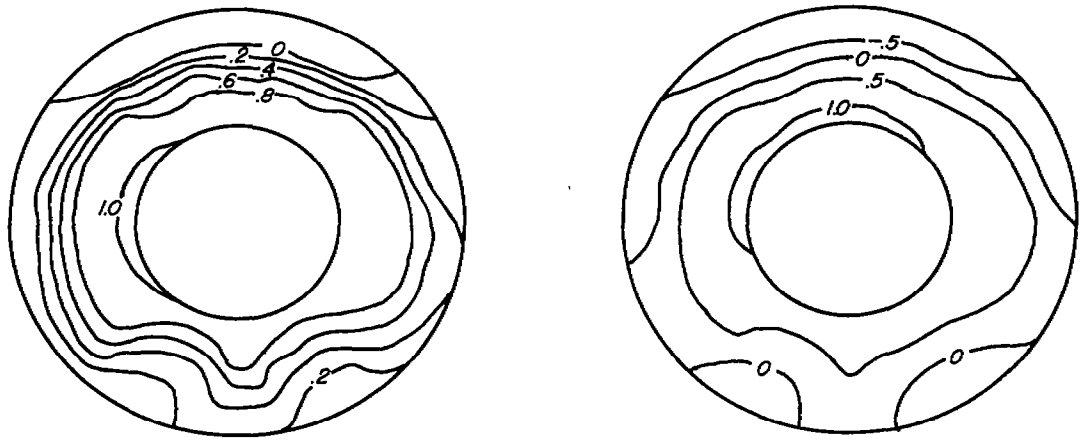

$\frac{m_1}{m_o} = 1.6$
$M_1 = 0.66$

$M_o = 0.33$

$\frac{m_1}{m_o} = 1.7$
$M_1 = 0.73$

NACA

(b) Rounded lip.

Figure 13.—Concluded.

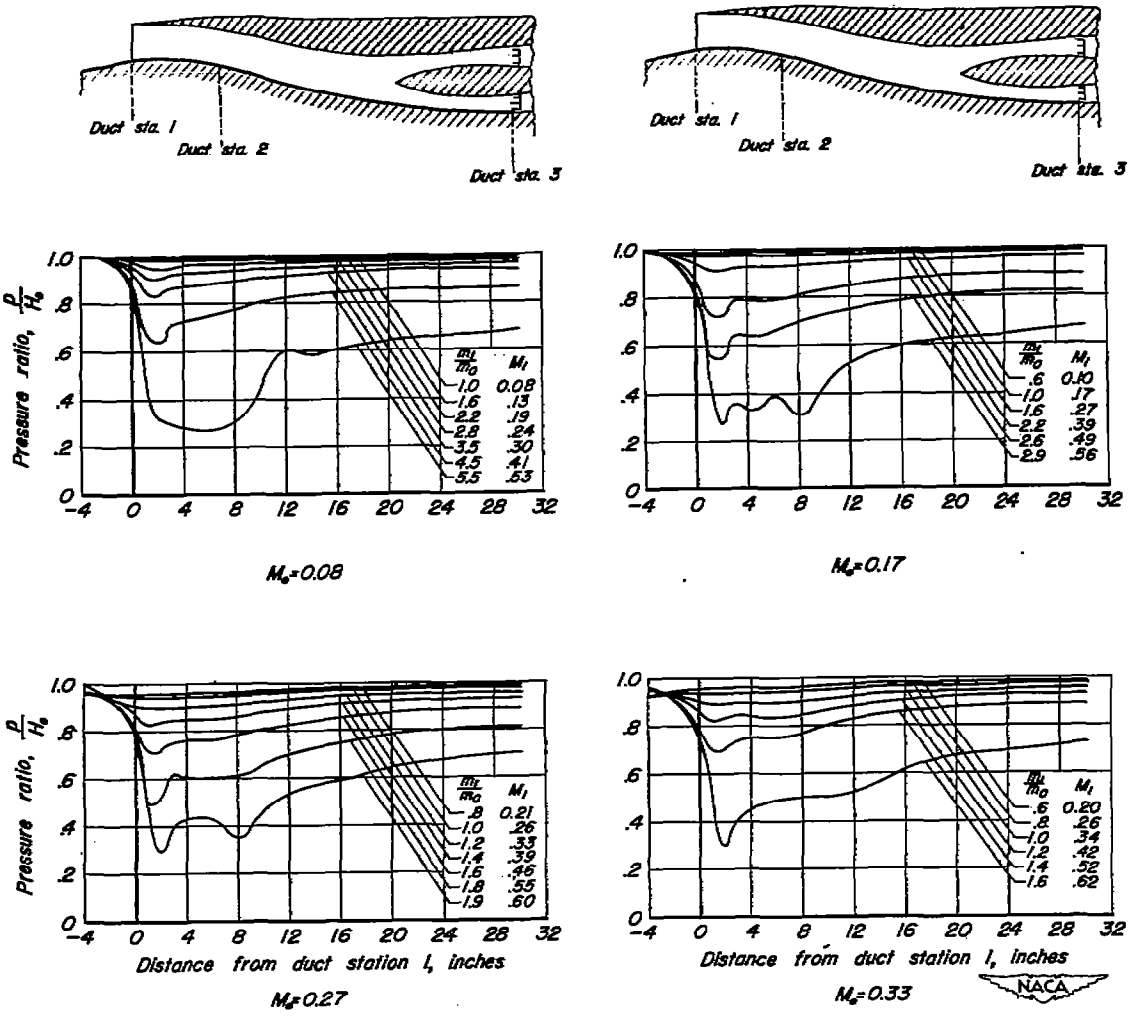

(a) Duct floor.

Figure 14.—Distribution of pressure ratio in the vertical plane of symmetry for the inlet having a sharp lip. $\alpha = 0°$.

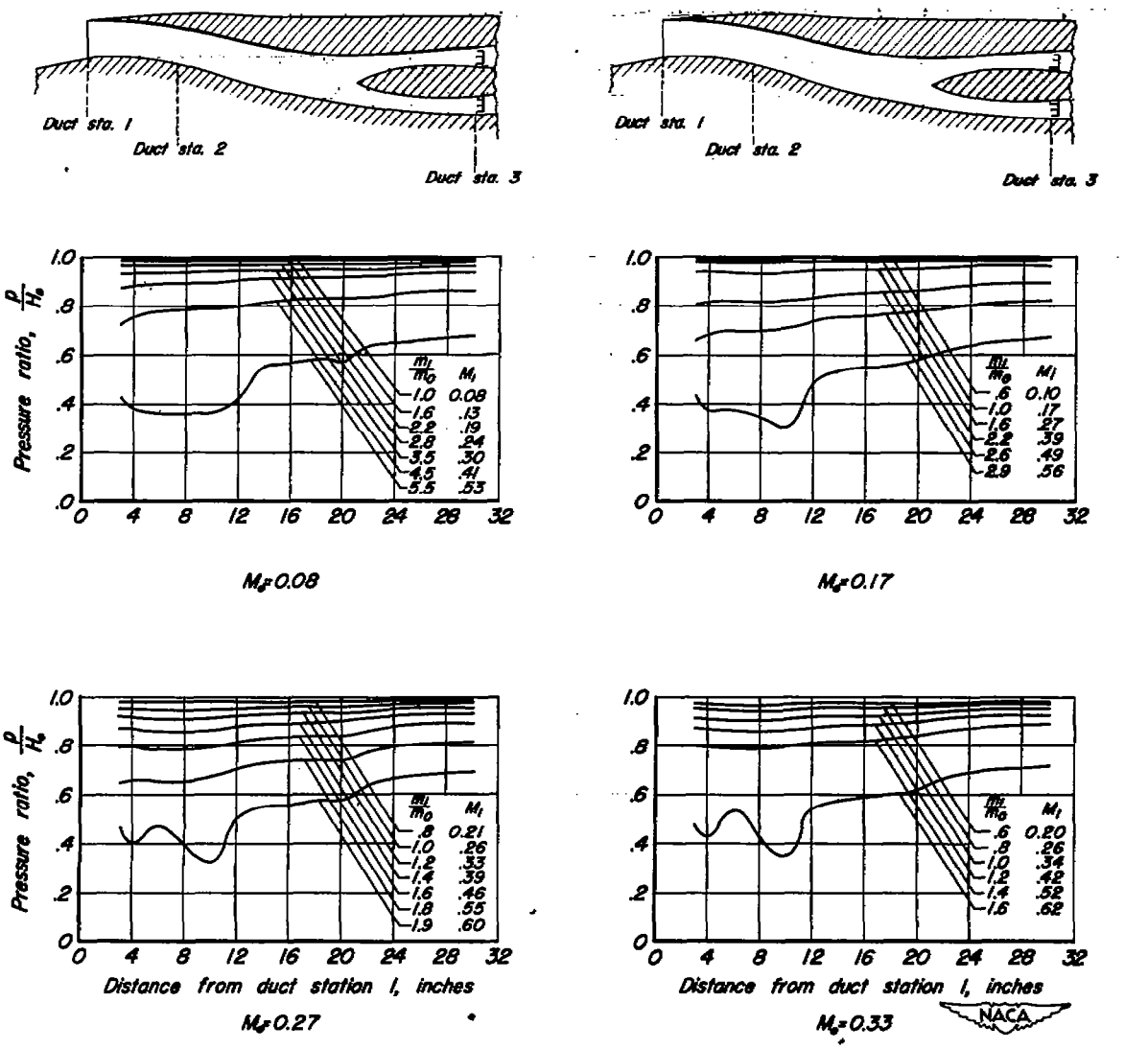

(b) Duct roof.

Figure 14.–Concluded.

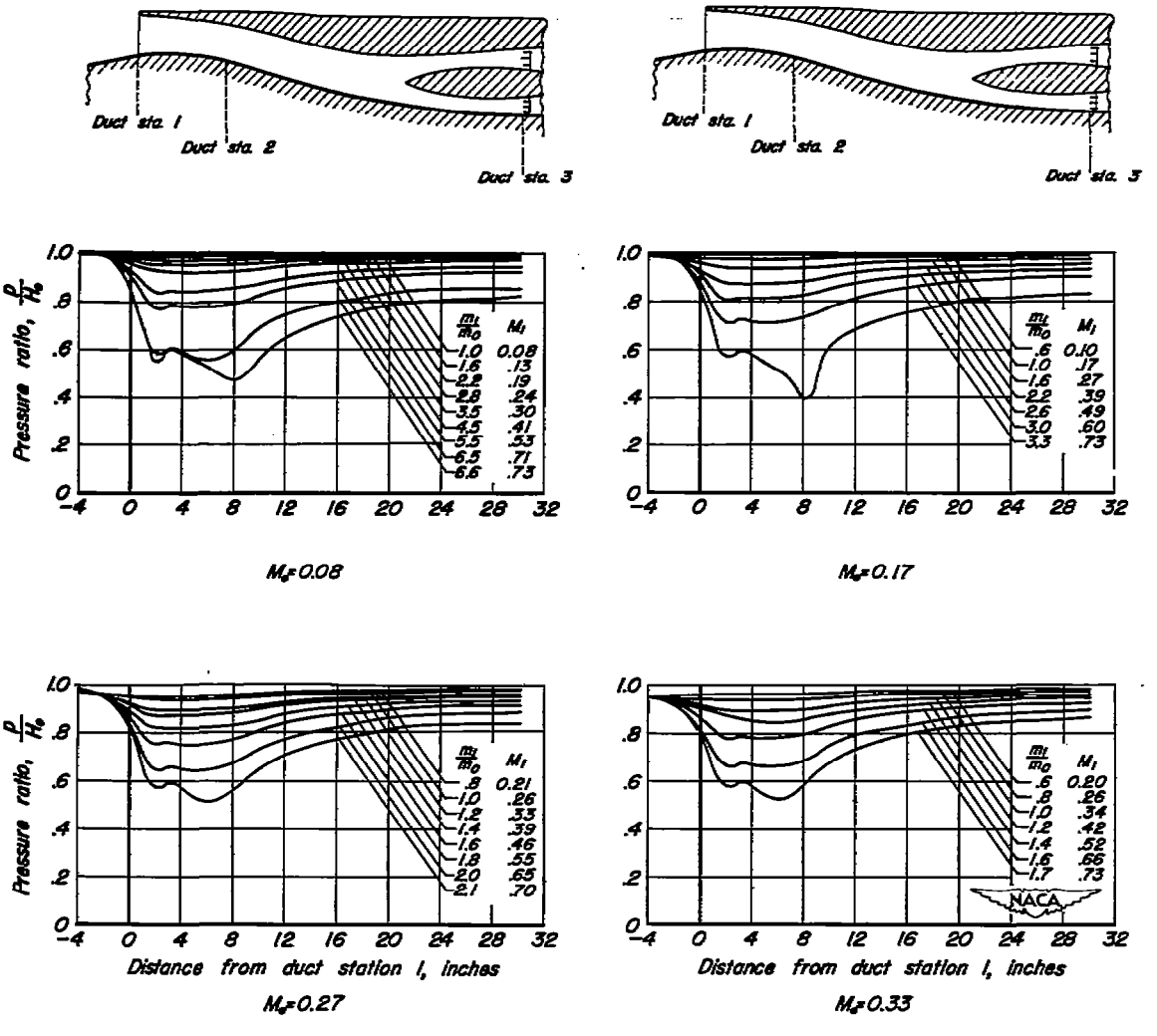

(a) Duct floor.

Figure 15.—Distribution of pressure ratio in vertical plane of symmetry for the inlet having a rounded lip. $\alpha = 0°$.

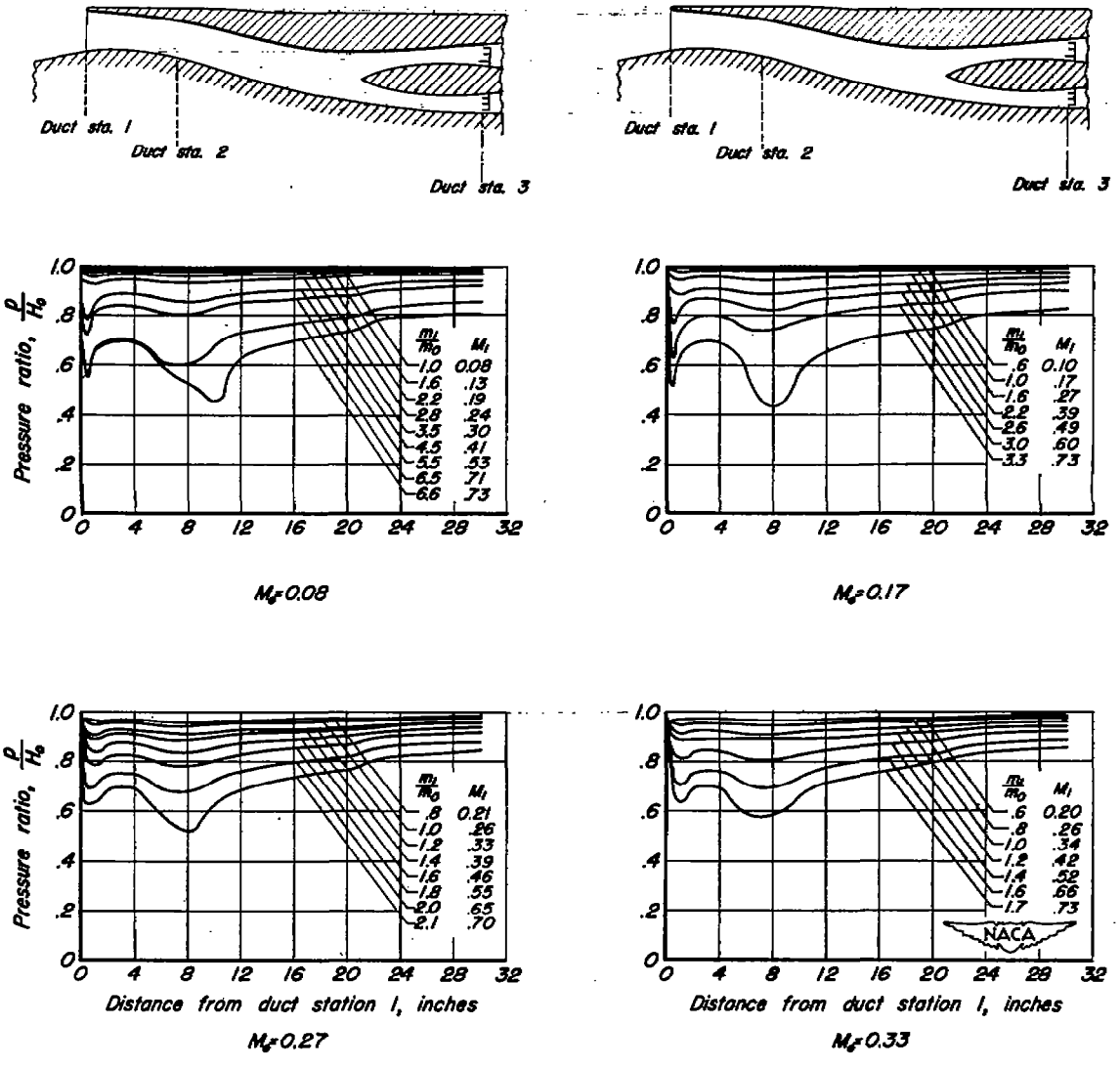

(b) Duct roof.

Figure 15.–Continued.

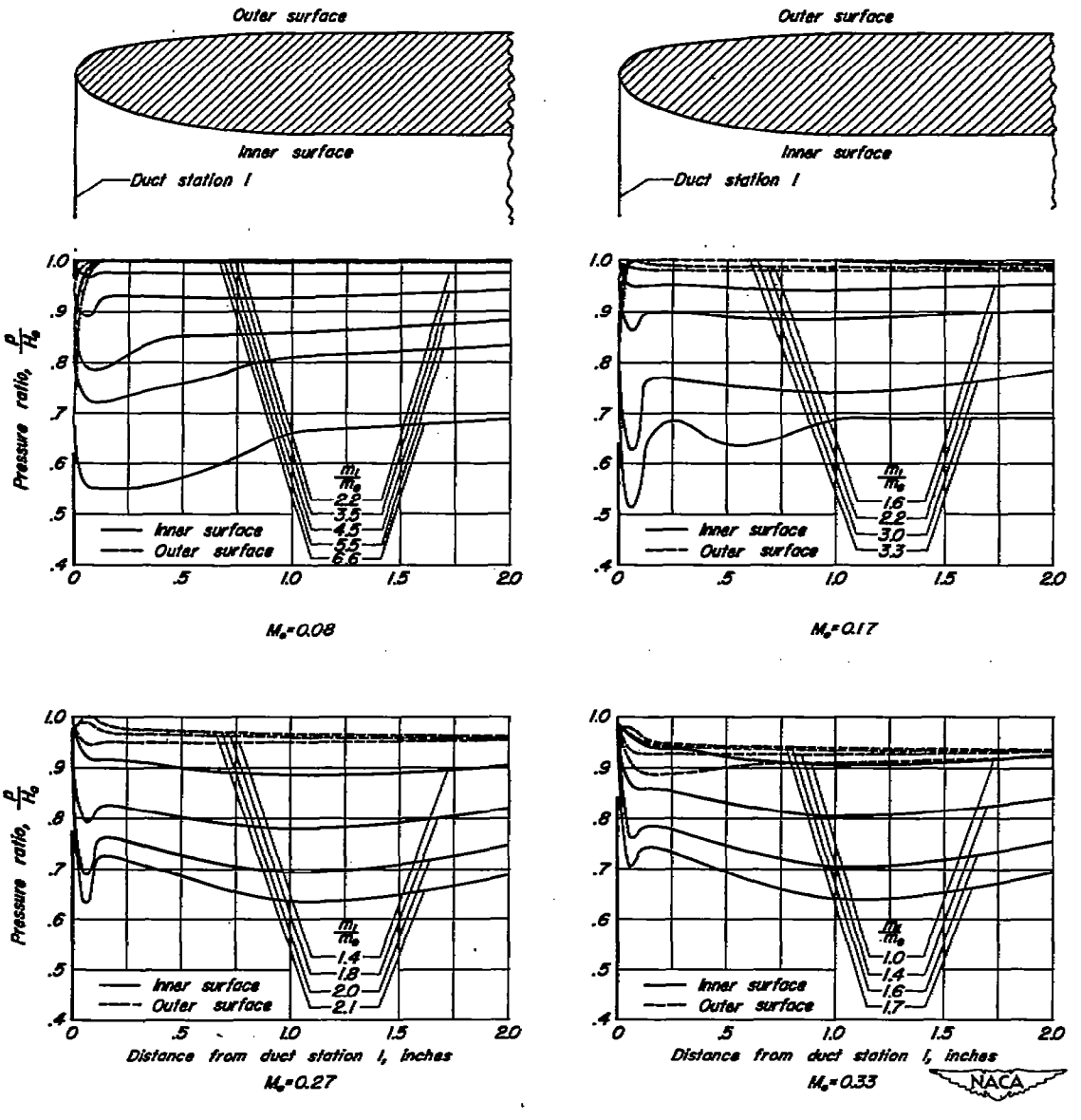

(c) Inner and outer surfaces of lip.

Figure 15.—Concluded.

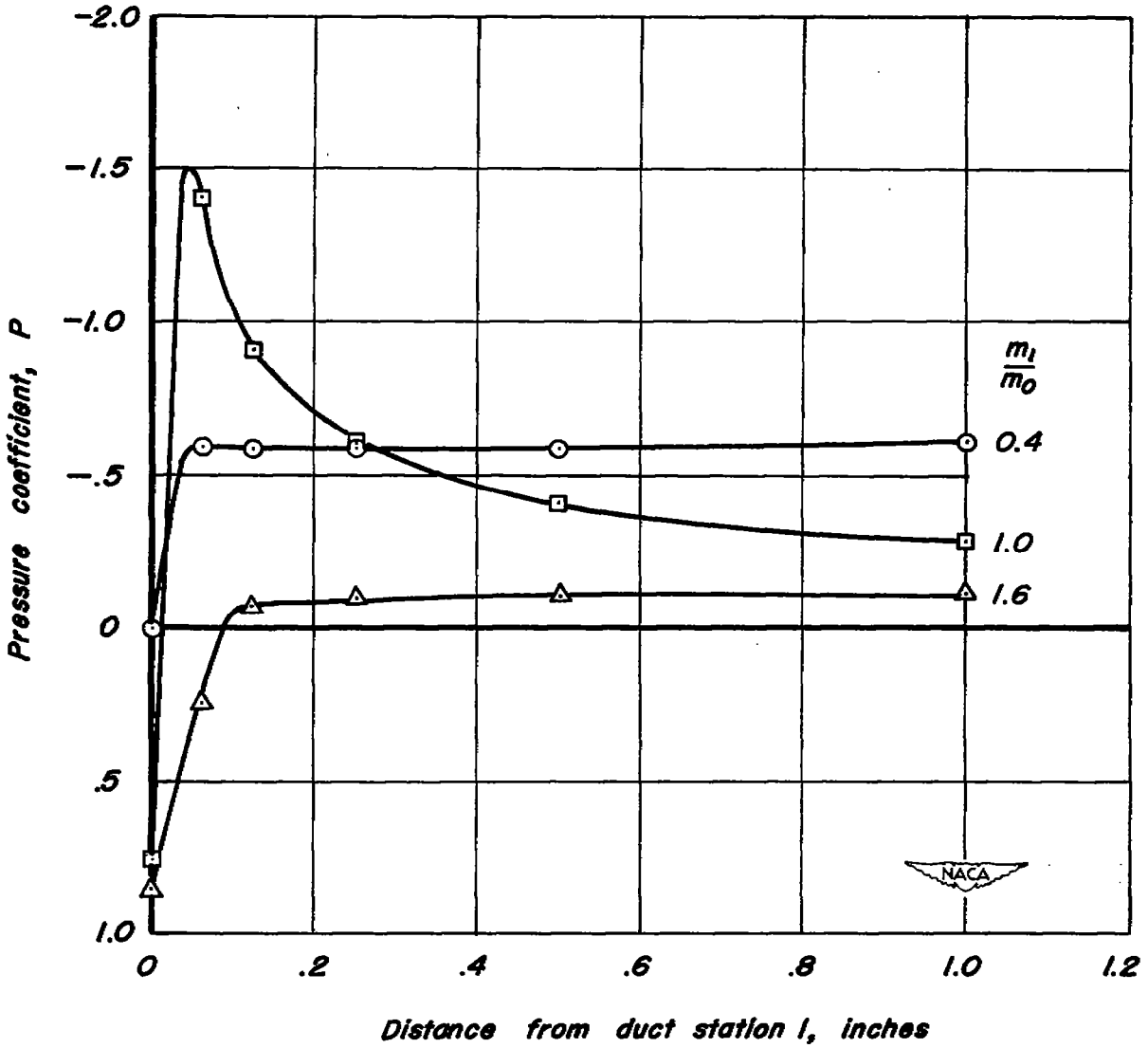

Figure 16.—Distribution of pressure coefficient on outer surface of the rounded lip. $M_0 = 0.17$, $\alpha = 0°$.

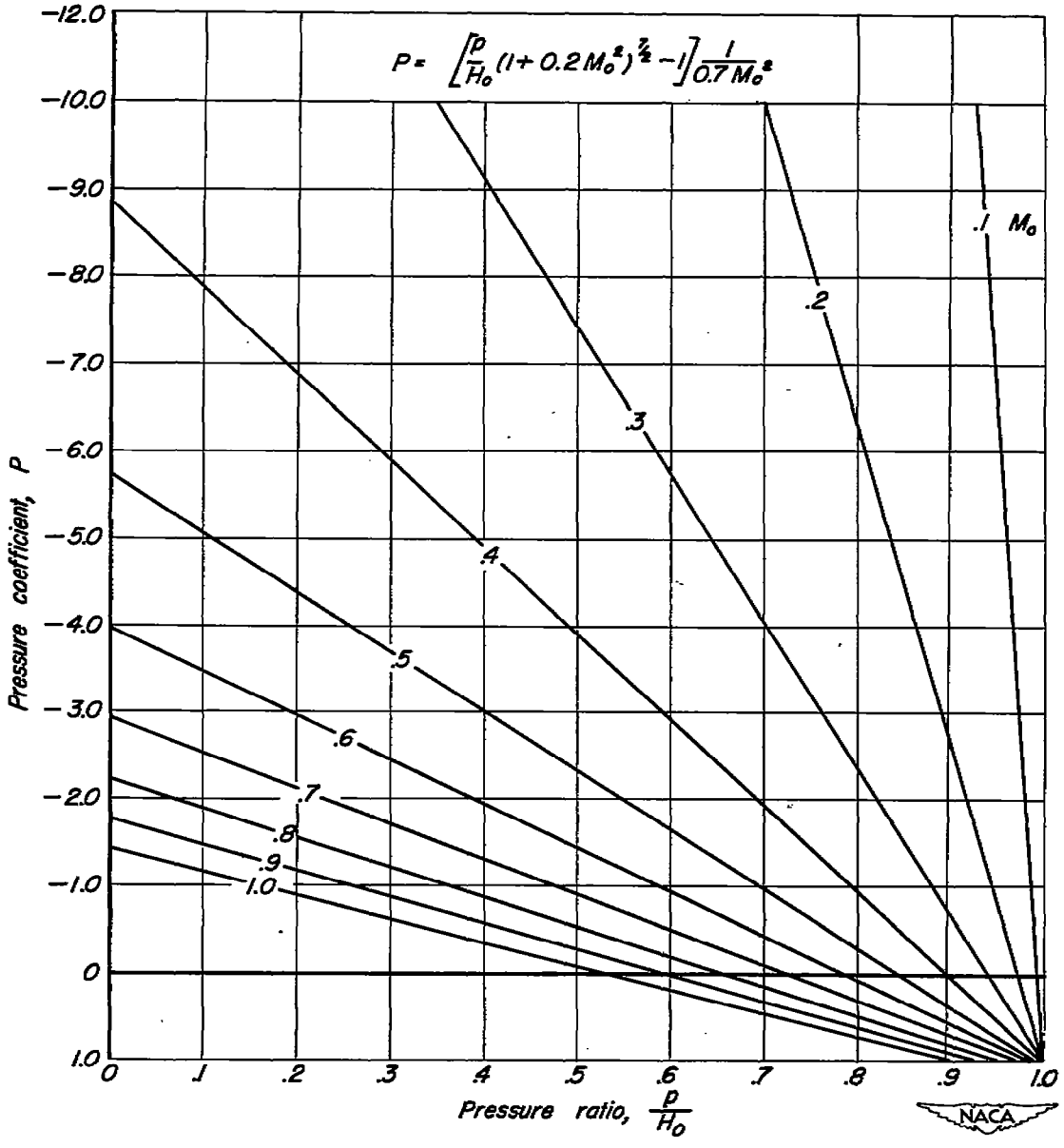

Figure 17.—Conversion of static-pressure coefficient to pressure ratio.

[redacted]

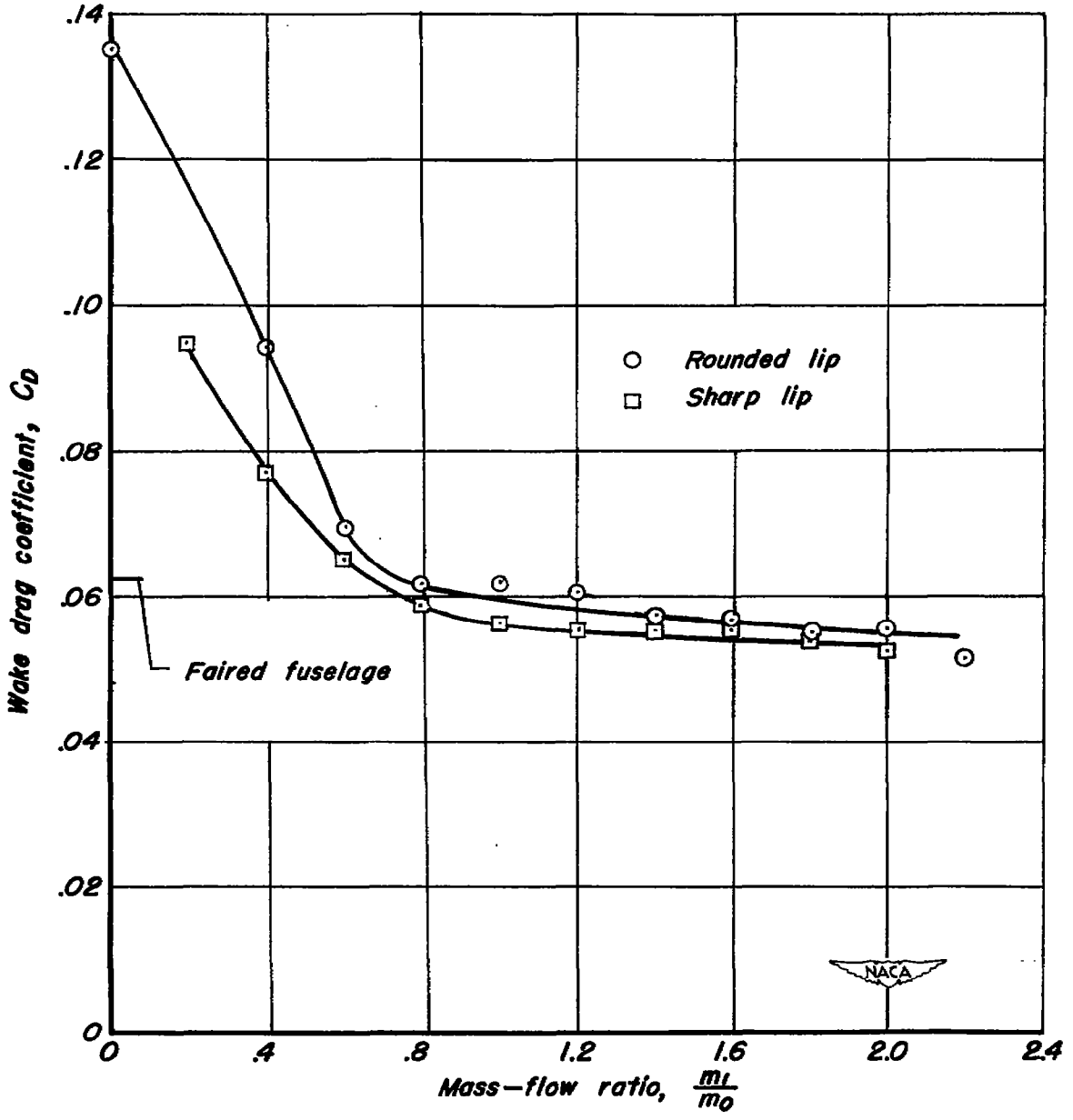

Figure 18.—The variation with mass-flow ratio of the wake drag coefficient of the forward portion of the fuselage. $M_0 = 0.24$, $\alpha = 0°$.

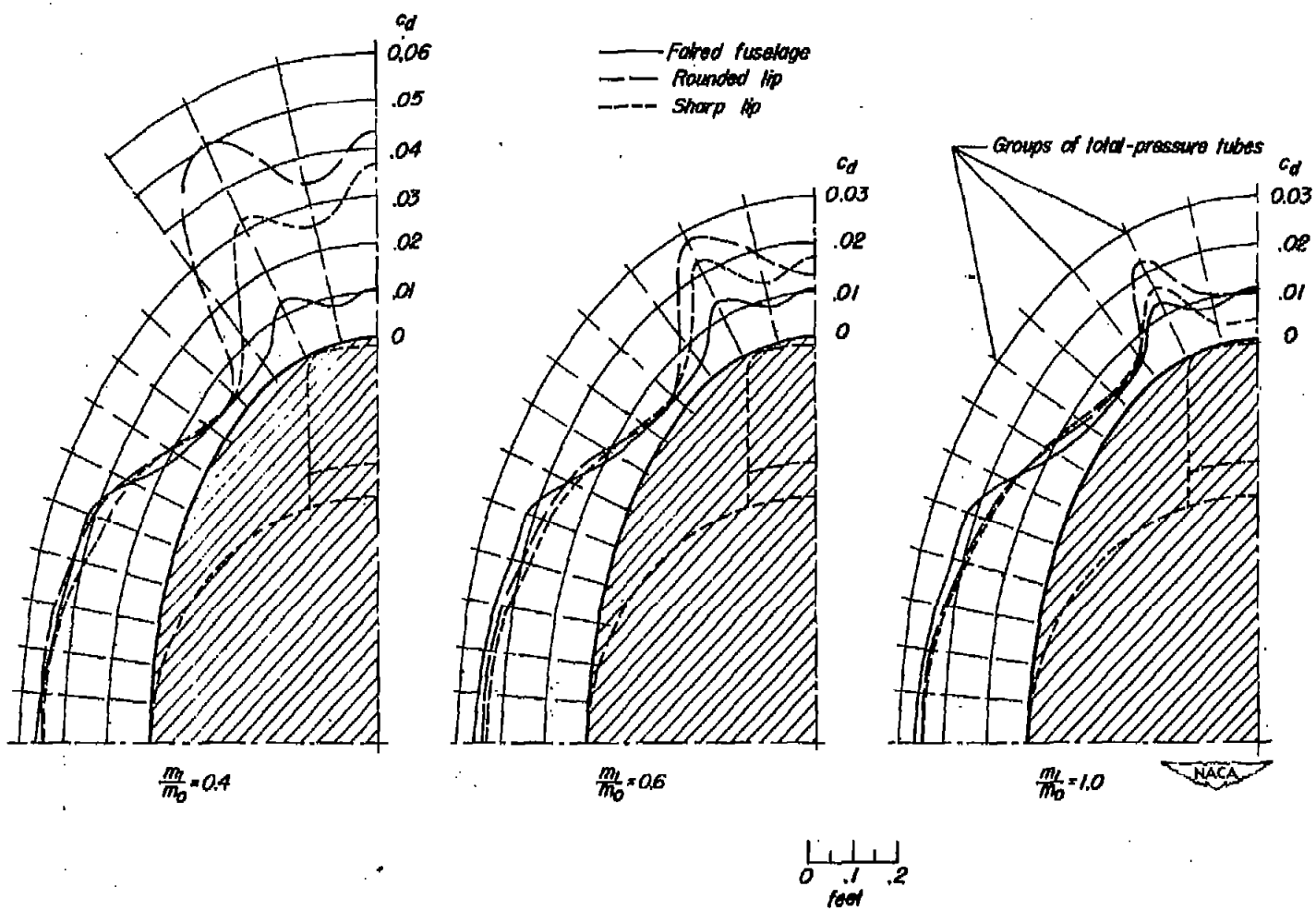

Figure 19.– Distribution of section wake drag coefficients at fuselage station 82 for three configurations. $\alpha = 0°$, $M_0 = 0.24$.